Bioorganic Chemistry 90 (2019) 103045

Contents lists available at ScienceDirect

Bioorganic Chemistry

journal homepage: www.elsevier.com/locate/bioorg

Novel Pyrazoloquinolin-2-ones: Design, synthesis, docking studies, and biological evaluation as antiproliferative EGFR-TK inhibitors

Mohammed A.I. Elbastawesy[a], Ashraf A. Aly[b,*], Mohamed Ramadan[a], Yaseen A.M.M. Elshaier[c], Bahaa G.M. Youssif[d], Alan B. Brown[e], Gamal El-Din A Abuo-Rahma[f,*]

[a] Department of Pharmaceutical Organic Chemistry, Faculty of Pharmacy, Al-Azhar University, 71524 Assiut, Egypt
[b] Department of Chemistry, Faculty of Science, Minia University, 61519 Minia, Egypt
[c] Department of Organic and Medicinal Chemistry, Faculty of Pharmacy, University of Sadat City, 32958 Menoufia, Egypt
[d] Department of Pharmaceutical Organic Chemistry, Faculty of Pharmacy, Assiut University, 71526 Assiut, Egypt
[e] Program in Chemistry, Florida Institute of Technology, Melbourne, FL 32901, USA
[f] Department of Medicinal Chemistry, Faculty of Pharmacy, Minia University, 61519 Minia, Egypt

ARTICLE INFO

Keywords:
Quinolin-2-one
Pyrazole
NCI
Antiproliferative
Molecular docking
EGFR-TK
Inhibitors

ABSTRACT

Two new series of diethyl 2-[2-(substituted-2-oxo-1,2-dihydroquinolin-4-yl)hydrazono]-succinates **6a-g** and 1-(2-oxo-1,2-dihydroquinolin-4-yl)-1*H*-pyrazole**s 7a-f** have been designed and synthesized. The structures of the synthesized compounds were proved by IR, mass, NMR (2D) spectra and elemental analyses. The target compounds were evaluated for their *in vitro* cytotoxic activity against 60 cancer cell lines according to NCI protocol. Consequently, seven compounds were further examined against the most sensitive cell lines, leukemia CCRF-CEM, and MOLT-4. 5-Amino-1-(6-bromo-2-oxo-1,2-dihydroquinolin-4-yl)-1*H*-pyrazole-3,4-dicarbonitrile (**7f**) was the most active product, with IC_{50} = 1.35 uM and 2.42 uM against MOLT-4 and CCRF-CEM, respectively. Also, it showed a remarkable inhibitory activity compared to erlotinib on the EGFR TK with IC_{50} = 247.14 nM and 208.42 nM, respectively. Cell cycle analysis of MOLT-4 cells treated with **7f** showed cell cycle arrest at G2/M phase (supported by Caspases, BAX and Bcl-2 studies) with a significant pro-apoptotic activity as indicated by annexin V-FITC staining. Moreover, the docking study indicated that both the pyrazole moiety and the quinolin-2-one ring showed good fitting into EGFR (PDB code: 1M17). In order to interpret SAR of the designed compounds, and provide a basis for further optimization, molecular docking of the synthesized compounds to known EGFR inhibitors was performed. The study illustrated the effect of several factors on the compounds' activity.

1. Introduction

Nitrogen containing heterocycles are indispensable structural units in medicinal chemistry. Among various heterocyclic compounds, the chemistry and biological applications of quinoline has been subjected to intense studies from different research groups [1,2]. Recently, quinazoline derivatives like gefitinib and erlotinib (Fig. 1) have been approved by the FDA as EGFR kinase inhibitors for the treatment of non-small cell lung and breast cancers [3–5]. Moreover, it was reported that the nitrogen atom at position-3 of the quinazoline core formed a water-mediated hydrogen bond with Thr^{766} (gatekeeper residue) within the EGFR pocket [6,7]. In contract, bioisosteric replacement of the quinazoline core with a quinoline ring afforded new quinoline derivatives such neratinib and pelitinib (Fig. 1), potent inhibitors of EGFR kinase [8–12]. This bioisosteric replacement did not require a water molecule to mediate the binding with the amino acid residue Thr^{766} [13]. Moreover, C-3-unsubstituted quinolines can give similar results; 2-styrylquinoline (**SQ-1**) derivatives (Fig. 1) have been reported as promising antitumor compounds against several tumor cell lines comparable to gefitinib [14–16].

The pyrazole framework is an exceptionally adaptable drug-like format that is being utilized broadly in the structure of cancer treatments and cellular apoptosis [17–19]. These compounds can exhibit anticancer activity by the restraint of various kinds of enzymes, proteins and receptors which assume basic roles in cell division [20]. Moreover, pyrazolo-fused compounds have been additionally developed as a significant heterocyclic framework because of their wide scope of biological activities [21–23], as well as synthetic applications in medicinal chemistry [24]. Pyrazoles were reported in a variety of potent anticancer active agents as Ruxolitinib (Fig. 1) [25] which were involved in

* Corresponding authors.
E-mail addresses: ashrafaly63@yahoo.com (A.A. Aly), gamal.aborahama@mu.edu.eg (G. El-Din A Abuo-Rahma).

https://doi.org/10.1016/j.bioorg.2019.103045
Received 1 April 2019; Received in revised form 5 June 2019; Accepted 5 June 2019
Available online 08 June 2019
0045-2068/

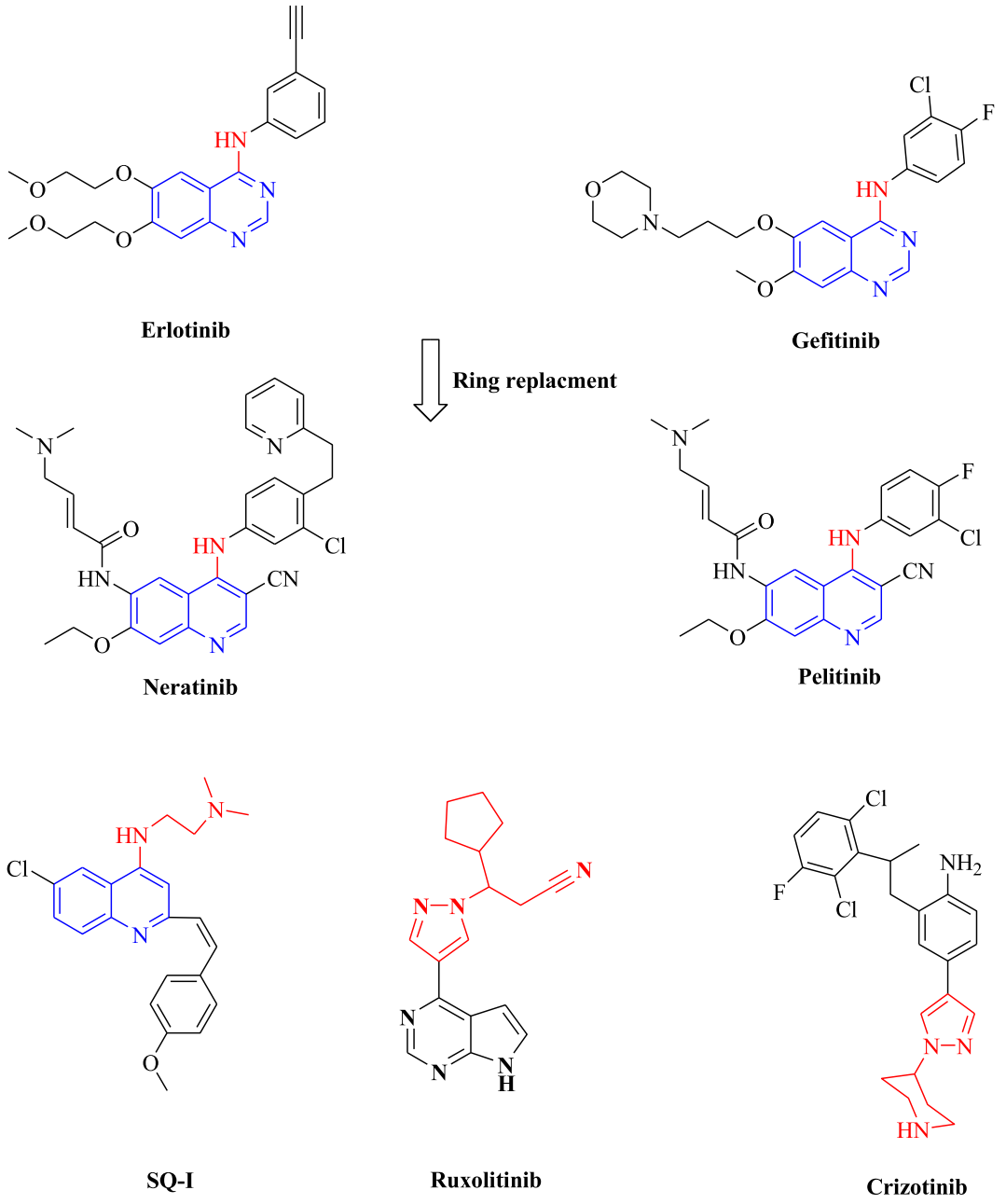

Fig. 1. Structure of different quinazoline, quinoline and pyrazole-based-anticancer agents.

the treatment of intermediate or high-risk myelofibrosis, a type of myeloproliferative disorder that affects the bone marrow [26,27]. Crizotinib, another pyrazole derivative, is an anticancer drug acting as an inhibitor of anaplastic lymphoma kinase (ALK) and c-ros oncogene 1 (ROS1), approved for treatment of some non-small cell lung carcinoma (Fig. 1) [28,29].

In recent years, pyrazolo-quinoline hybrids **PQ-1** and **PQ-2** (Fig. 2) have been reported as potent antitumor agents [30,31].

In our previous studies, we synthesized ethyl pyrano[3,2-*c*]quinoline-4-carboxylates [32], spiro(indoline-3,4′-pyrano[3,2-*c*]-quinoline)-3′-carbonitriles [33], 2,3-bis(4-hydroxy-2-oxo-1,2-dihydroquinolin-3-yl) succinates, and arylmethylene-bis-3,3′-quinoline-2-ones [34]. Besides, two series of *N*-2,3-bis(6-substituted-4-hydroxy-2-oxo-1,2-dihydroquinolin-3-yl)naphthalene-1,4-diones and substituted *N*-(methyl/ethyl)bis-quinolinone triethyl-ammonium salts were successfully synthesized. The synthesized compounds were targeted as candidates to extracellular signal-regulated kinases 1/2 (ERK1/2) with considerable antineoplastic activity [35]. Moreover, we reported on the design and synthesis of novel series of fused naphthofuro[3,2-*c*]quinoline-6,7,12-triones and pyrano[3,2-*c*]quinoline-6,7,8,13-tetraones as potential ERK inhibitors. The newly prepared inhibitors were evaluated for their ability to inhibit ERK1/2 in an *in vitro* radioactive kinase assay. Some of these compounds were found to inhibit ERK1 with IC_{50} of 0.5 and 0.19 μM, and inhibited ERK2 with IC_{50} of 0.6 and 0.16 μM respectively. Kinetic mechanism studies revealed that the inhibitors are ATP-competitive inhibitors where other inhibited ERK2 with a K_i of 0.09 μM [36].

In view of the above mentioned findings and our previous success in screening the antitumor activities of quinolones [35,36], the aim of this research became the synthesis of new quinoline bio-conjugates of potential EGFR inhibitory and anticancer properties. Our drug design strategy was based upon optimizing the bio-active hits by manipulation of the lead compound **PQ-1** (Fig. 2) through the following:

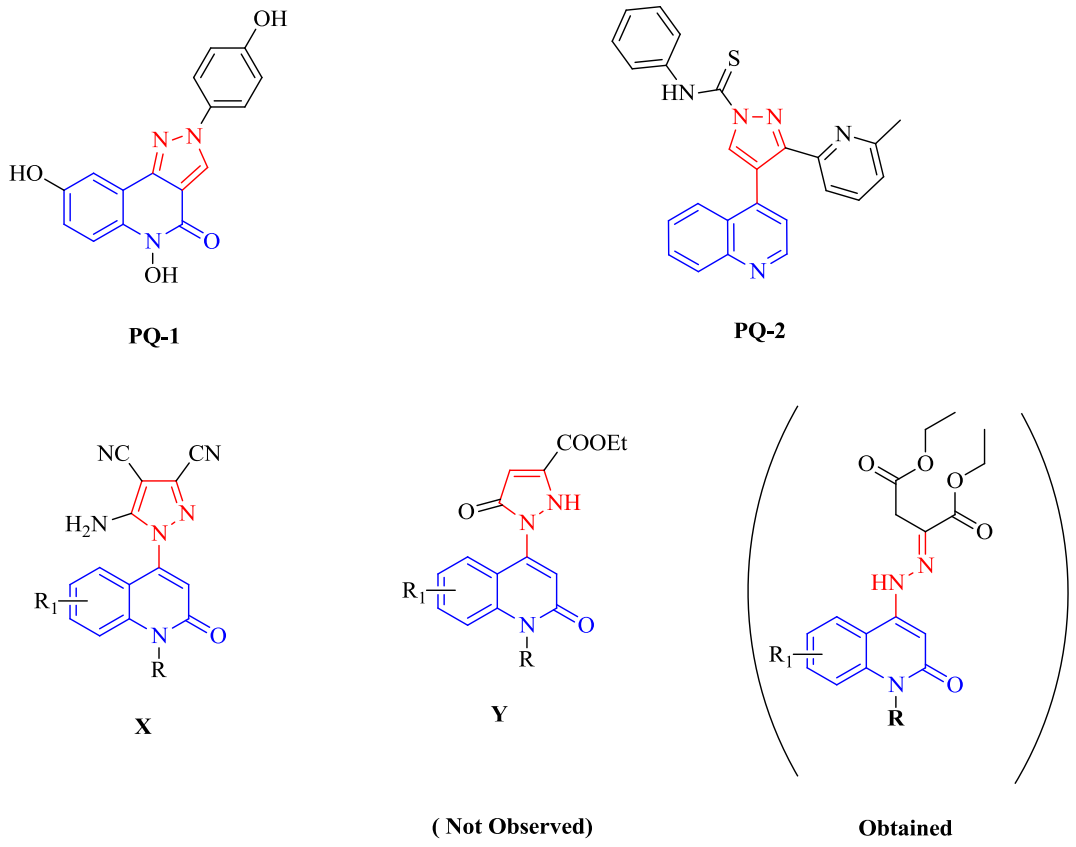

Fig. 2. Structure of different anticancer pyrazolo-quinoline hybrids and the target compounds.

(a) Molecular hybridization of quinolin-2-one with pyrazole to form designed structures **7a-f** and **Y** that included pyrazole nucleus which is an important pharmacophore;
(b) Replacing the lateral phenyl group in **PQ-1** by carbonitrile and amino functional groups able to form hydrogen bonds with EGFR receptors, and test their antitumor activity against different tumor cell lines.

Accordingly, two new series of 1-(2-oxo-1,2-dihydroquinolin-4-yl)-1*H*-pyrazole**s (7a-f)** and 5-Oxo-1-(2-oxo-quinolin-4-yl)-1*H*-pyrazole-3-carboxylic acid ethyl ester **(Y)** have been designed. Detailed biological studies were carried out on the newly synthesized pyrazole-quinoline conjugates to test their activities as an EGFR inhibitor and as antitumor active agents. Attempted synthesis of **Y** led to by-products **6a-g,** which were tested as open-chain analogues of pyrazoles **7**.

2. Results and discussion

2.1. Chemistry

The target compounds **6a-g** and **7a-f** were prepared according to Scheme 1. Compounds **1–5** were synthesized according to the literature [37–39], and their structures were confirmed by matching their spectral data with those reported [39]. The key intermediates, 4-hydrazino-quinolin-2-ones **5a-g,** were prepared by heating at reflux compounds **4a-g** with hydrazine hydrate for 12 h [39]. To our surprise, refluxing **5a-g** with diethyl acetylene dicarboxylate (**DEAD**) in DMF furnished diethyl 2-(2-(subsituted-2-oxo-1,2-dihydroquinolin-4-yl)hydrazono) succinates **6a-g** instead of pyrazoles **Y**. The spectral and elemental data results revealed that all derivatives **5a-g** underwent the reaction smoothly to give the respective open structures **6a-g** in 74–90% yield.

Reagent and reaction conditions: (a) Diethyl malonate, PPA, reflux 3 h; (b) $POCl_3$, reflux 2 h; (c) AcOH, reflux 10 h; (d) $NH_2NH_2{\cdot}H_2O$ (85%), EtOH, reflux 8 h; (e) **DEAD**, DMF, Et_3N, reflux 10–16 h; (f) **TCNE**, EtOH, reflux 20–24 h.

The IR spectra of **6a-g** showed an absorption band at 3328–3215 cm^{-1} corresponding to the NH group, and bands at 1743–1731 cm^{-1} characteristic of the ester C=O. In addition, absorptions at 2992–2975 and 1675–1630 cm^{-1} are characteristic of C=N, respectively. As an example, the ^{1}H NMR spectra of **6a,** for example, showed two sets of ethoxy signals, immediately excluding the cyclic pyrazole structure, which would have only one**.** All the 19 Hs showed HSQC correlation with either a C or an N, confirming that they belong to the sample under analysis, not a solvent or water. In addition to the ethoxy groups, there are two NH protons, a four-spin aromatic system, a 1H vinylic singlet at δ_H 6.34 and a 2H singlet at δ_H 3.97. The latter singlet is assigned as H-4e (Table 1). These two protons correlated with both ester carbonyls at δ_C 168.28 and 163.94, assigned as C-4f and C-4i respectively; with a carbon at δ_C 135.30, assigned as C-4d; and with an sp^2 nitrogen at δ_N 342.4, assigned as N-4c. The assignments of H-4e, C-4e, C-4d, and N-4c require that the oxaloacetate subunit exist as an imino tautomer not an enamine (Table 1).

The mass spectra and elemental analyses indicated that the molecular weight is consistent with the molecular formula of the open chain analogue. Scheme 2 suggests the mechanism of formation of such compounds as due to nucleophilic attack of the lone pair of electrons of NH_2-hydrazine to the acetylenic bond to give intermediate **A** (Scheme 2). Neutralization of intermediate **A** would give **B**, which on proton transfer would give **6a-g** (Scheme 2). Similar mechanisms have been reported [33,36,40,41].

On other hand, heating at reflux compounds **5a-f** with ethene-1,1,2,2-tetracarbonitrile (**TCNE**) in ethanol furnishes the corresponding 1-(2-oxo-1,2-dihydroquinolin-4-yl)-1*H*-pyrazole**s 7a-f** in moderate yields. Elemental analyses, IR and NMR in addition to mass spectra were in good agreement with the assigned product structures. As a representative example for this series, the IR spectrum of compound **7d**

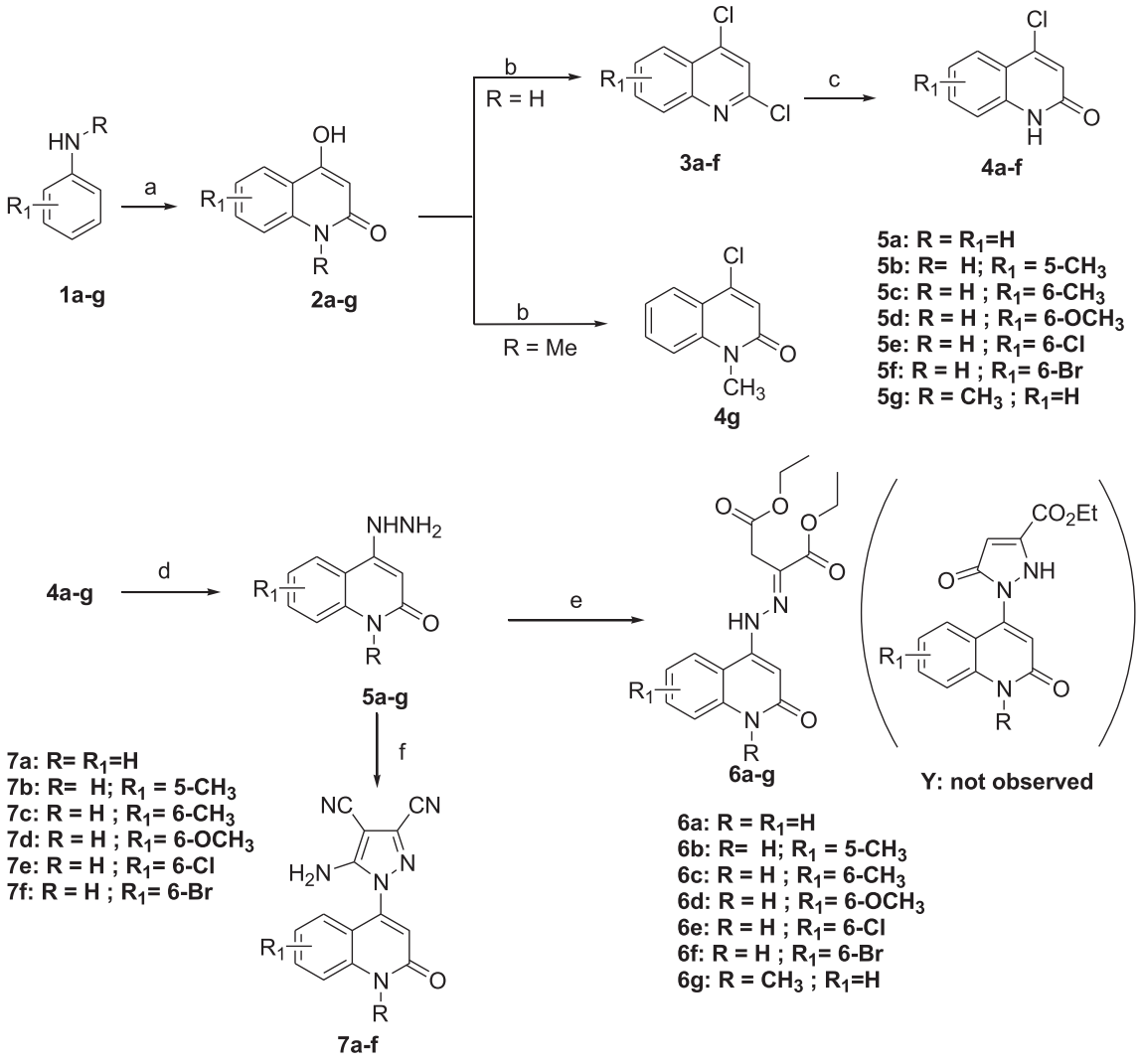

Scheme 1. Synthesis of target compounds **6a-g** and **7a-f.**

showed frequencies corresponding to amino, nitrile and C═N groups at ν 3347, 3196 (NH_2), 2227 (CN), 1674 (C═N) cm^{-1}, respectively. Moreover, the ^1H NMR spectrum of **7d** showed a broad singlet signal at δ_H 7.56 (disappeared upon deuteration) representing NH_2 protons; their attached nitrogen appears at δ_N 62.8, and gives HMBC correlation with two carbons in the pyrazole ring not with the quinolone. In addition, there is a characteristic singlet signal at δ_H 3.38 related to OCH_3 group. The ^{13}C NMR spectrum of **7d** showed two peaks at δ_C 111.95 and 111.91 assigned to the cyano groups, a signal at δ_C 126.90 for C═N, and a peak at δ_C 160.70 assigned to the C═O of the quinolone moiety (Table 2).

Mass spectra and elemental analyses data confirmed the suggested structural formula.

The formation of the pyrazole structure can be explained as due to nucleophilic attack of the lone pair of electrons of NH_2-hydrazine to the ethylene bond to give intermediate **C** (Scheme 3). Neutralization and elimination of a molecule of HCN from intermediate **C** would give **D**. Subsequently, nucleophilic attack of the lone pair of electrons of the NH-hydrazine atom to the carbonitrile carbon would give Zwitter-ion **E**. Ultimately; neutralization of **E** would give **F**, which on aromatization would give **7a-f** (Scheme 3).

2.2. Biology

2.2.1. Evaluation of in vitro antiproliferative activity for compounds 6a-g and 7a-f

The target compounds **6a-g** and **7a-f** were selected by the National Cancer Institute [NCI, Bethesda, MD, USA (http://www.dtp.nci.nih.gov.)] for evaluation at a single concentration of 10 μM towards a panel of sixty cancer cell lines of nine diverse tissues according to NCI protocol. The screening results were reported (Figs. 3 and 4, Table 3) as the percent growth of treated cells compared to untreated control cells. The cyclized 1-(2-oxo-1,2-dihydroquinolin-4-yl)-1*H*-pyrazole compounds **7a-f** are more active than the open chain analogues containing hydrazino-succinic acid diethyl ester backbone **6a-g**, which reflects a positive influence of cyclization on the antiproliferative activity. 1-(2-Oxo-1,2-dihydroquinolin-4-yl)-1*H*-pyrazole scaffold compounds **7a-f** showed promising activities against a majority of the tested cancer cell lines. Substituents attached to the phenyl moiety affected the activity: it was found that compounds **7e** and **7f**, possessing 6-chloro and 6-bromo substituents respectively, were more active against all tested leukemia cancer cell lines than compound **7d** with a 6-methoxy substituent, which showed no inhibitory effect against any of the tested leukemia cell lines. A similar pattern was also observed to PC-3 prostatic cancer

Table 1
NMR spectroscopic assignments of compound **6a** (italicized correlations are weak).

^{1}H NMR:		COSY:	Assignment:	
11.38 (s; 1H)			H-1	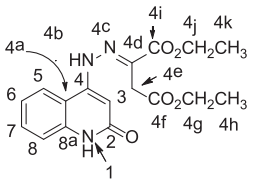
10.07 (s; 1H)			H-4b	
8.14 (d, *J* = 8.0; 1H)		*7.54,* 7.21	H-5	
7.54 ("t", *J* = 7.3; 1H)		*8.14,* 7.33, 7.21	H-7	
7.33 (d, *J* = 8.0; 1H)		7.54	H-8	
7.21 (dd, *J* = 7.8, 7.3; 1H)		8.14, 7.54	H-6	
6.34 (s; 1H)			H-3	
4.25 (q, *J* = 7.1; 2H)		1.29	H-4j	
4.12 (q, *J* = 7.1; 2H)		1.20	H-4g	
3.97 (s; 2H)		H-4e		
1.29 (t, *J* = 7.1; 3H)		4.25	H-4k	
1.20 (t, *J* = 7.1; 3H)		4.12	H-4h	
^{13}C NMR:	**HSQC:**	**HMBC:**		**Assignment:**
168.28		4.12, 3.97		C-4f
163.94		4.25, 3.97		C-4i
162.33				C-2
148.13		10.07, 8.14, *7.33,* 6.34		C-4
139.36		8.14, 7.54		C-8a
135.30		10.07, 3.97		C-4d
130.80	7.54	8.14, *7.21*		C-7
122.95	8.14	7.54		C-5
120.76	7.21	7.33		C-6
115.62	7.33	7.54, 7.21		C-8
111.93		11.38, *10.07,* 8.14, *7.54,* 7.33, 7.21, 6.34		C-4a
99.13	6.34	*11.38,* 10.07		C-3
61.04	4.25	1.29		C-4j
60.73	4.12	1.20		C-4g
32.12	3.97			C-4e
14.08	1.29	4.25		C-4k
13.98	1.20	4.12		C-4h
^{15}N NMR	**HSQC:**	**HMBC:**	**Assignment:**	
342.4		10.07, 3.97	N-4c	
145.1	11.38	*7.33*	N-1	
141.6	10.07	6.34	N-4b	

6a

cell line and HOP-92 non-small cell lung cancer. Here, the halogen bearing compound **7e** showed excellent cell growth inhibition activity against HOP-92 non-small cell lung cancer and PC-3 prostatic cancer cell line with a high GI values of −79.6% and −87.3%, respectively; **7f** resembled **7e,** with GI values of −90.8% and −86.9%, but the methoxy-bearing **7d** gave GI values of 35.29 and 10.65%, respectively (Table 3). On the other hand, compounds **6a-g** showed moderate cytotoxic activities against majority of cancer cell lines. Among them, compounds **6d**, **6e** and **6f** have good anticancer activity against all the tested leukemia cell lines.

It is obvious that the electronic effect and the position of substituent on the tested scaffolds had a pronounced effect on their cytotoxic activity. Compounds **6d-f** with electron withdrawing groups on the pendant phenyl group showed higher antiproliferative activity with GI values 73.91% (**6d**) and lethal effect −0.31% (**6e**) and −15.7% (**6f**) against MOLT-4 leukemia cell line than compounds **6b** and **6c** with electron donating groups (GI = 0 and 81.67%, respectively) (Table 3). Compared with 6-substituted **6c**, the 5-substituted **6b** showed no inhibitory effect against all the tested leukemia cell lines, indicating the importance of the 6-substitution for optimizing activity where a similar trend was also observed in case of PC-3 prostatic cancer cell line. From the results, it is clear that substitution on the phenyl group of quinolone is important for the antiproliferative activity where the most active compounds against all of the tested leukemia cell line are substituted at position 6, compared to the unsubstituted analogues (**6d-f** *vs* **6a**).

2.2.2. *In vitro five dose full NCI 60 cell panel assay*

Compounds **7e** and **7f** were selected for five dose testing against the full panel of 60 human tumor cell lines according to NCI protocol (http://www.dtp.nci.nih.gov.), Appendix A.

Compound **7e** exhibited noteworthy antiproliferative activity against ovarian cancer cell lines with GI_{50} = 8.63 μM (Table 4) and selectivity ratio = 4.99, and against non-small cell lung cancer with GI_{50} = 11.35 and selectivity ratio = 3.79. Compound **7f** showed

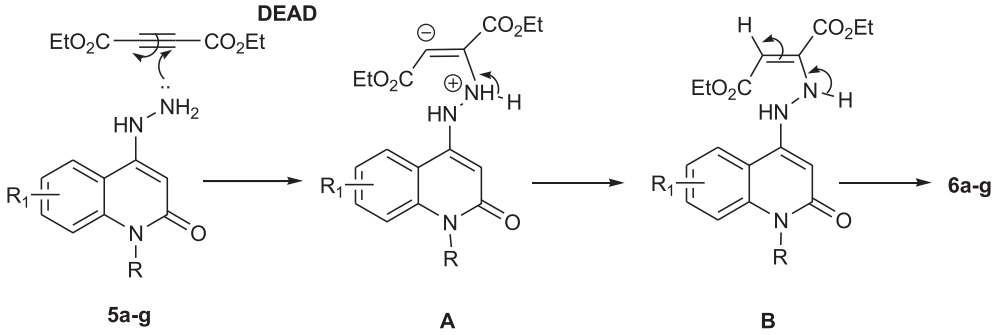

Scheme 2. Mechanism for the formation of compounds **6a-g.**

Table 2
NMR spectroscopic assignments of compound **7d** (italicized correlations are weak).

^{1}H NMR	^{1}H–^{1}H COSY:	Assignment:	
12.13 (s; 1H)	6.81	H-1	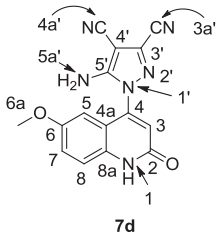
7.56 (bs; 2H)		H-5a′	
7.39 (d, *J* = 9.7; 1H)	7.31, 6.58	H-7	
7.31 (d, *J* = 8.8; 1H)	7.39, 6.58	H-8	
6.81 (s; 1H)	12.13, 6.58	H-3	
6.58 (s; 1H)	7.39, 7.31, 6.81	H-5	
3.38 (s; 3H)	12.13	H-6a	
^{13}C NMR:	HSQC	HMBC	Assignment:
160.77			C-2
154.50		7.39, 7.31, 6.81, 6.58, 3.72	C-6
152.99		7.56	C-5′
142.25		7.39, *7.31,* 6.81, 6.58	C-4
134.16		7.39, 7.31, 6.58	C-8a
126.90			C-3′
122.72	6.81	*12.13*	C-3
120.60	7.31	6.58	C-7
117.21	7.39		C-8
116.38		12.13, 7.39, 7.31, 6.81	C-4a
111.95, 111.91			C-3a′, 4a′
105.38	6.58	7.39, 7.31, 6.81	C-5
75.86		7.56	C-4′
55.62		3.72	C-6a
^{15}N NMR:	HSQC:	HMBC:	Assignment:
189.0		7.56, 6.81	N-1′
151.6	12.13	7.39, 6.81	N-1
62.8	7.56		N-5a′

7d

antiproliferative activity against ovarian cancer cell lines with GI_{50} = 37.90 μM and selectivity ratio = 1.29, and against non-small cell lung cancer with GI_{50} = 22.27 and selectivity ratio = 2.21.

$$\textbf{Selectiveindex} = \frac{\textbf{MIDa}}{\textbf{MIDb}}$$

2.2.3. Effect of compounds 6c-f, 7b, 7e and 7f on MOLT-4 and CCRF-CEM leukemia cancer cells growth

Seven compounds **6c-f**, **7b**, **7e** and **7f** were evaluated for their anticancer activity against MOLT-4 and CCRF-CEM leukemia cancer cell lines by MTT assay (Appendix A) [42]: the results are shown in Table 5**.** Compounds **7b**, **7e** and **7f**, with the 1-(2-oxo-1,2-dihydroquinolin-4-yl)-1*H*-pyrazole scaffold, showed better anticancer activity than open chain analogues **6c-f**. Compounds **7e** and **7f** with 6-chloro and 6-bromo substitution on the quinoline core were found the most potent against tested cancer cell lines showing IC_{50} of 4.34 ± 0.14 μM and 1.35 ± 0.08 μM, respectively against MOLT-4 where the standard erlotinib showed IC_{50} = 07.38 ± 0.56 μM. The same pattern was observed against the CCRF-CEM leukemia cell line (Table 5). Compounds **7e** and **7f** substituted at 6-position showed better activity against the MOLT-4 leukemia cell line (IC_{50} 4.34 ± 0.14 μM for **7e**, and 1.35 ± 0.08 μM for **7f**) than compounds **6e** and **6f** bearing the same substitution at 6-position but with hydrazino-succinic acid diethyl ester backbone (IC_{50} = 11.34 ± 0.22 μM for **6e** and 7.57 ± 0.16 μM for **6f)**. Finally, it is noteworthy that compound **6c**, with 6-methyl substitution on the quinoline core, was found to be the least potent among the tested compounds against the MOLT-4 line, with IC_{50} 43.19 ± 0.71 μM.

In short, the presence of cyclized pyrazole at position 4 of quinolone gave much better activity than the open scaffold at the same position against the majority of the tested cancer cell lines. Moreover, substitution at the quinolone 6 position with electron withdrawing groups like Br or Cl enhances greatly the anticancer activity, while introduction of an electron-donating 6-methyl group reduces activity greatly. Similarly, shift of the substituent into position 5 of the quinolone moiety abolished activity (*cf*. **6b** and **6c**).

2.2.4. EGFR TK inhibitory activity

The mechanism at molecular level of the most active antiproliferative compounds **6e**, **6f**, **7b**, **7e** and **7f** were investigated on EGFR TK kinase (Table 6) [43]. The findings of the cancer cell-based assays have been powerfully complemented by the results from the EGFR assay. Compounds **7e** and **7f** showed potent EGFR inhibition with IC_{50} 298.27 and 247.14 nM, respectively while that of erlotinib was 208.42 nM. Compound **6e** displayed the least potent activity (IC_{50} = 703.84 nM) among all the tested compounds. The inhibitory effect against EGFR TK kinase is consistent with their antiproliferative

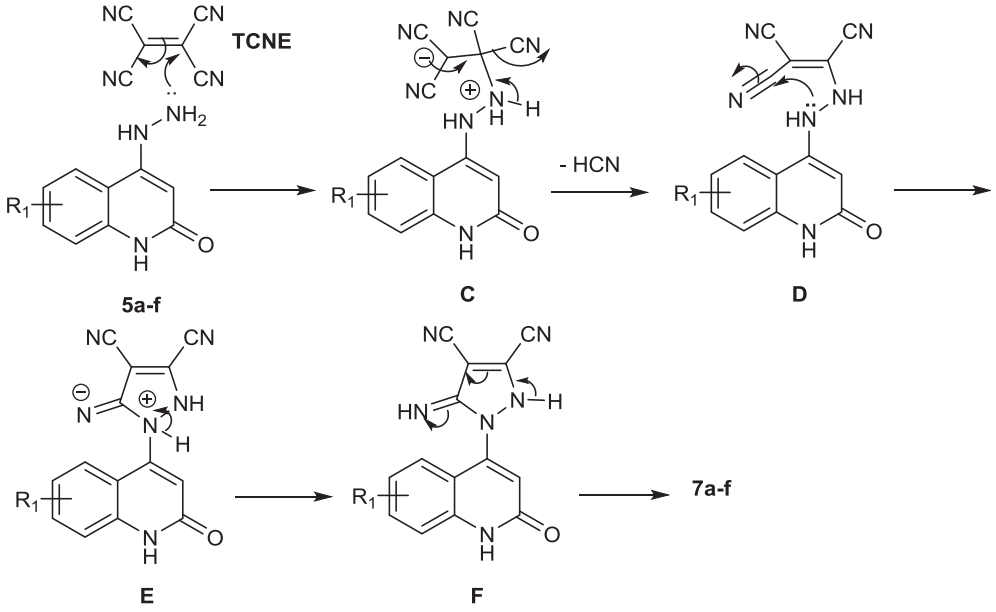

Scheme 3. Mechanism for the formation of compounds **7a-f.**

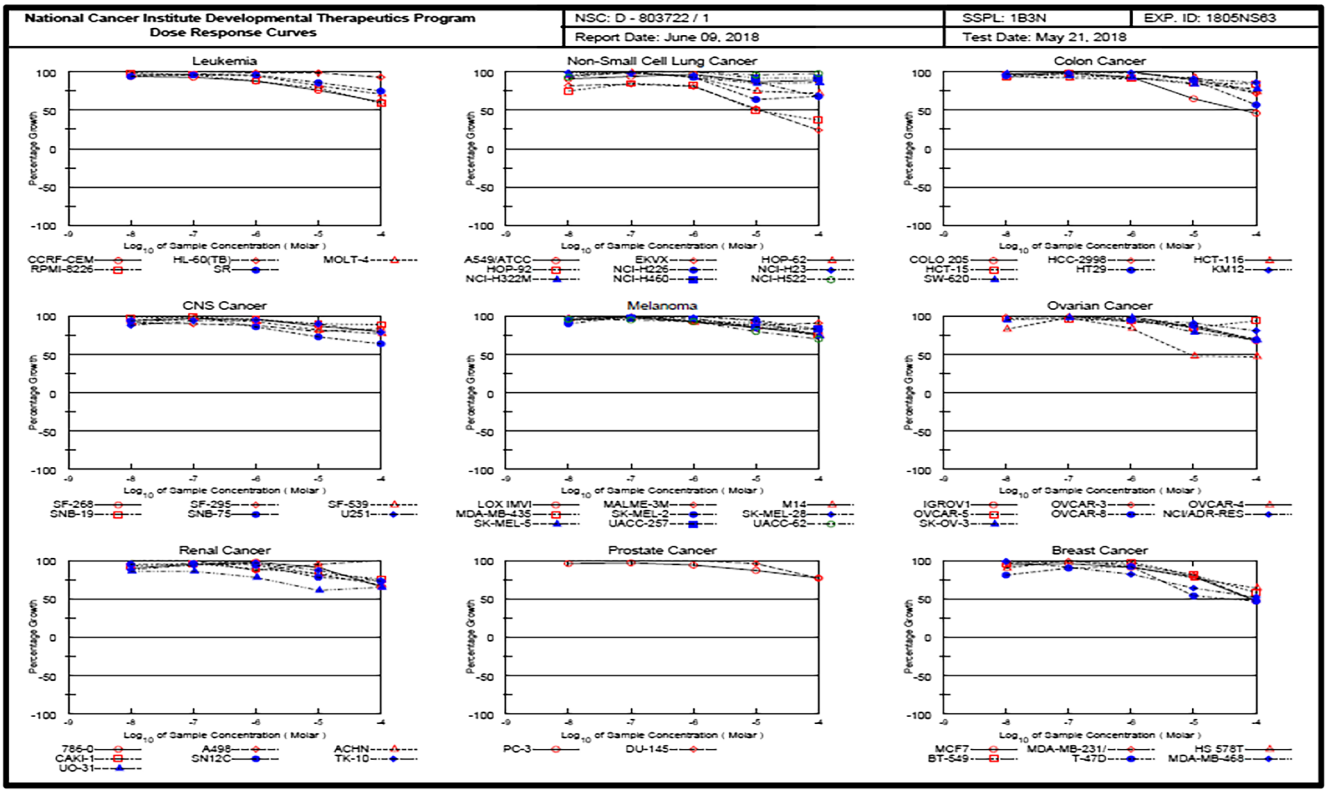

Fig. 3. Dose-antiproliferative response of compound **7e** against nine different cancer cell lines.

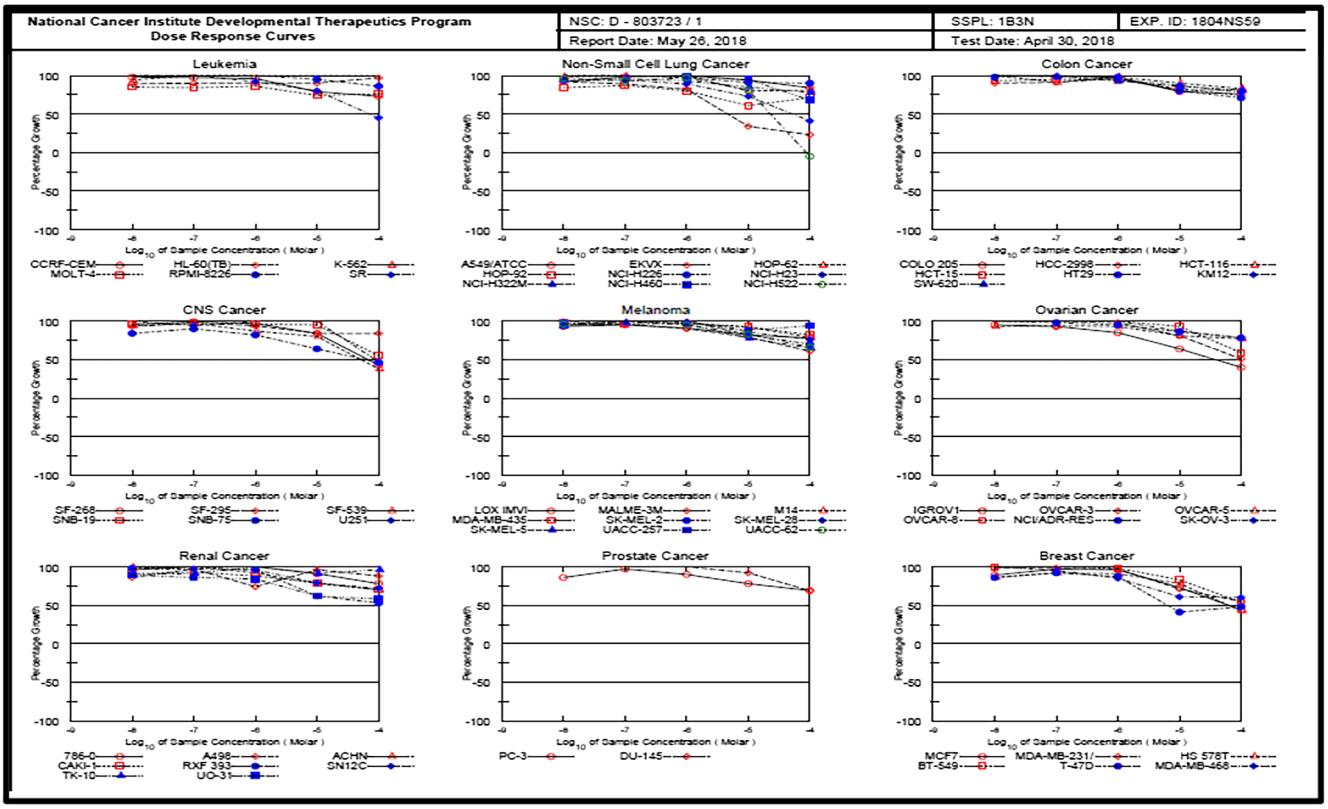

Fig. 4. Dose-antiproliferative response of compound **7f** against nine different cancer cell lines.

Table 3
Percentage growth inhibition (GI %) of *in vitro* subpanel tumor cell lines at 10 mM concentration for compounds **6a-g** and **7a-f**.

Subpanel cancer cell Lines	% Growth Inhibition (GI %)[a]												
	6a	6b	6c	6d	6e	6f	6 g	7a	7b	7c	7d	7e	7f
Leukemia													
CCRF-CEM	–	–	−57.19	−47.5	−51.5	−36.7	–	–	11.44	28.73	–	−15.8	–32.0
HL-60(TB)	–	–	–	–	–	−7.48	–	13.77	–	–	–	99.03	−11.2
K-562	–	–	10.56	10.69	56.05	75.85	–	28.23	24.05	10.71	–	−43.9	−12.4
MOLT-4	–	–	81.67	73.91	−0.31	−15.7	–	12.41	–	–	–	−3.9	−16.1
RPMI-8226	–	–	–	31.45	42.82	16.79	–	10.89	–	–	–	−24.6	−29.7
SR	–	–	53.64	33.01	53.04	59.20	–	25.37	–	–	–	99.29	−14.2
Non-small cell lung cancer													
A549/ATCC	–	–	–	–	–	–	–	–	–	–	–	–	–
EKVX	–	–	–	–	–	–	–	–	32.15	–	–	–	12.53
HOP-62	–	–	–	–	–	–	–	12.78	31.86	17.29	13.67	12.81	16.81
HOP-92	–	–	20.17	12.82	12.52	23.85	10.55	–	15.70	–	35.29	−79.6	−90.8
NCI-H226	–	–	–	–	–	13.13	12.62	14.59	21.32	–	–	–	–
NCI-H23	–	–	–	–	–	–	–	14.56	11.09	–	–	–	–
NCI-H322M	–	–	–	–	–	–	–	–	33.20	–	–	–	–
NCI-H460	–	–	–	–	–	–	–	–	18.93	–	–	–	–
NCI-H522	–	–	–	–	–	–	11.45	18.59	22.97	22.18	10.98	12.90	21.63
Colon cancer													
COLO 205	–	–	–	–	–	–	–	–	–	–	–	–	20.04
HCC-2998	–	–	–	–	–	–	–	37.15	–	–	–	–	21.53
HCT-116	–	–	–	–	–	–	–	–	24.02	13.52	12.95	15.61	14.27
HCT-15	–	–	–	–	–	–	–	–	12.13	–	–	–	–
HT29	–	–	–	–	–	–	–	–	–	–	–	–	–
KM12	–	–	–	–	–	–	–	–	–	–	–	–	–
SW-620	–	–	–	–	–	–	–	–	–	–	–	–	16.47
CNS cancer													
SF-268	–	–	–	–	–	–	–	–	–	–	–	–	–
SF-295	–	–	–	–	–	–	–	–	–	–	–	–	–
SF-539	–	–	–	–	–	–	–	–	10.20	–	–	–	–
SNB-19	–	–	–	–	–	–	–	–	11.39	–	–	–	–
SNB-75	10.30	–	–	–	–	11.77	17.55	–	–	–	–	–	12.74
U251	–	–	–	–	–	–	–	–	13.56	–	–	–	–
Melanoma													
LOX IMVI	–	11.06	–	–	–	–	–	–	18.98	–	–	–	–
MALME-3M	–	–	–	–	–	–	–	20.47	21.79	15.69	–	–	10.57
M14	–	–	–	–	–	–	–	–	15.11	–	–	–	–
MDA-MB-435	–	–	–	–	–	–	–	–	–	–	–	–	–
SK-MEL-2	–	–	–	–	–	–	–	–	–	–	–	–	–
SK-MEL-28	–	–	–	–	–	–	–	–	–	–	–	–	–
SK-MEL-5	–	–	–	–	–	–	–	–	–	–	–	–	–
UACC-257	–	–	–	–	–	–	–	–	12.12	–	11.73	13.03	–
UACC-62	–	12.64	–	–	–	–	–	22.08	19.75	12.96	13.97	18.06	13.41
Ovarian cancer													
IGROV1	–	–	–	–	–	17.41	–	24.71	35.93	11.26	14.50	–	–
OVCAR-3	–	–	–	–	–	–	–	–	–	–	–	–	–
OVCAR-4	–	12.63	–	–	–	–	–	–	10.97	10.8	–	–	18.37
OVCAR-5	–	–	–	–	–	–	–	–	–	–	–	–	–
OVCAR-8	–	–	–	–	–	–	–	–	14.09	10.59	–	–	–
NCI/ADR-RES	–	–	–	–	–	–	–	–	–	–	–	–	–
SK-OV-3	–	–	–	–	–	–	–	12.84	25.54	21.67	21.72	25.42	30.92
Renal cancer													
786-0	–	–	–	–	–	–	–	–	14.75	10.39	–	–	–
A498	–	–	–	–	–	–	–	–	–	–	–	–	–
ACHN	–	–	–	–	–	–	–	13.40	16.87	–	–	–	–
CAKI-1	15.27	12.94	–	–	–	16.86	10.36	–	17.42	–	–	–	–
RXF 393	–	–	–	–	–	–	–	–	–	–	–	–	–
SN12C	–	–	–	–	–	–	–	–	23.63	–	–	–	12.75
TK-10	–	–	–	–	–	–	–	–	–	–	–	–	–
UO-31	19.52	27.67	13.32	21.87	16.29	28.62	10.49	38.76	54.77	23.63	28.38	24.15	34.26
Prostate cancer													
PC-3	–	–	–	10.98	11.73	12.59	–	–	28.88	13.89	10.65	−87.3	−86.9
DU-145	–	–	–	–	–	–	–	–	–	–	–	–	–
Breast cancer													
MCF7	–	–	–	12.13	–	–	–	–	14.91	–	–	–	–
MDA-MB-231/ATCC	–	–	–	–	–	–	–	15.58	14.51	–	–	–	14.72
HS 578 T	–	–	–	–	–	–	–	–	–	–	–	–	11.41
BT-549	–	–	–	–	–	–	–	–	13.11	–	13.47	12.07	14.89
T-47D	–	–	–	–	–	–	–	14.41	22.95	21.08	11.25	32.76	43.91

(*continued on next page*)

Table 3 (*continued*)

Subpanel cancer cell Lines	% Growth Inhibition (GI %)[a]												
	6a	6b	6c	6d	6e	6f	6 g	7a	7b	7c	7d	7e	7f
MDA-MB-468	–	–	–	10.94	–	–	–	–	–	13.91	–	–	–

(–): Weak activity GI < 10%.

effects, where the cyclized 5-amino-1*H*-pyrazole 3,4-dicarbonitrile compounds are superior in activity when compared with the open chain analogues. This study demonstrates that compounds **7e** and **7f** are strong inhibitors of EGFR and can probably be promising anticancer agents.

2.2.5. Activation of caspases cascade

Activation of caspases plays a key role in the initiation and effecting of the apoptotic process [44]. Among the most common caspases, caspase-3 is an essential player that cleaves multiple proteins in the cells, leading to apoptotic cell death [45]. The effect of compounds **7e** and **7f** on caspase 3 were evaluated and compared to erlotinib as a reference drug. Compounds **7e** and **7f** showed an increase in the level of active caspase 3 by 5.14 and 5.82 fold versus control, respectively, compared to erlotinib (6.49 fold) as shown in Table 7. Moreover, the effects of compounds **7e** and **7f** on caspases 8 and 9 was also evaluated; compound **7e** increases the levels of caspases 8 and 9 by 2.82 and 10.10 fold respectively, while compound **7f** increases their level by 3.52 and 9.63 fold, respectively, compared to erlotinib (6.52 and 11.15 fold respectively: Table 7). Thus, both **7e** and **7f** are potential activators of both intrinsic and extrinsic caspase pathways with more prominent effect on the intrinsic pathway, since caspase 9 levels are higher.

2.2.6. Effects on BAX and Bcl-2 proteins.

Bcl-2 (B-cell lymphoma 2) family members are significant regulators of apoptosis that can be classified into three groups. The first group protects against apoptosis (Bcl-2 itself). The second group of proteins is represented by Bax (Bcl-2 associated protein X) and Bak (Bcl-2 antagonist/killer), which are the key activators of the apoptosis machinery in response to cellular stress stimuli. The third group is comprised of different categories of proteins such as Bid (BH3 interacting death domain), Bim (Bcl-2 interacting mediator) and others [46]. Overexpression of the antiapoptotic Bcl-2 members leading to antagonizing apoptosis and development of resistance of tumor cells to common chemotherapeutic agents. Thus, the development of new drugs that can inhibit the action of antiapoptotic Bcl-2 members is a very attractive strategy in the design of anticancer agents [47]. The effect of compounds**7e** and **7f** on the expression levels of Bcl2 and BAX was determined after treatment of MOLT-4 cells with the IC_{50} of compounds**7e** and **7f** (Table 8). Compound **7e** caused up-regulation in the level of the proapoptotic protein BAX approximately five-fold while it markedly down-regulated the levels of the antiapoptotic proteins Bcl2 up to four-fold compared to the control untreated cells. Compound **7f** caused up-regulation in the level of the BAX over four-fold whiles it markedly down-regulated the levels of the antiapoptotic proteins Bcl2 three-fold compared to the control. These findings proved the proapoptotic effect of compounds **7e** and **7f**.

2.2.7. Cell cycle analysis and apoptosis assay

2.2.7.1. Cell cycle analysis. The cell cycle includes four phases: The G1 phase where cell enlargement and preparation of DNA duplication occurs; the S phase (synthesis) is the stage of DNA replication and chromatid duplication; in G2 Phase, repairing of new DNA and more growth occurs while in the M stage nuclear division takes place. Studies on the effect of compound **7f** on cell cycle development and induction of apoptosis in the MOLT-4 were done. MOLT-4 was incubated with IC_{50} concentration of compound **7f** for 24 h. Consequently, the cell line was stained with PI/Annexin V and analyzed by flow cytometry using BD FASCC alibur [48]. Investigation of the results in Fig. 5, exposed that percentage of pre G1 apoptosis induced by **7f** on MOLT-4 was 22.42%. A high percent of cell accumulation was observed in G2-M phase in MOLT-4 treated with compound **7f** after 24 h incubation, indicating arrest of cell cycle at G2-M phase.

2.2.7.2. Apoptosis assay. Cell cycle analysis of MOLT-4 after treatment with compound **7f** showed presence of pre-G1 peak which is an indication of apoptosis. To confirm the ability of **7f** to induce apoptosis, cells were stained with Annexin V/PI, incubated for 24 h and analyzed. Analysis of early and late apoptosis showed that compound **7f** was able to induce significant levels of apoptosis with necrosis percent 4.61 and 15.32, respectively (Figs. 6 and 7) and that % of necrosis was 2.49.

2.3. Docking study

A library of the target compounds, structurally related compounds (Figs. 1 and 2), and known EGFR inhibitors (Erlotinib and Gefitinib) was designed and energy minimized using MMFF94 force field calculations. The catalytic domain of EGFR (PDB code: 1M17) [49] was prepared for docking using Open Eye® software. Docking was conducted using the Fred application and the data was visualized by the Veda application. This software package generates consensus scoring which is a filtering processes to obtain virtual binding affinity: a lower consensus score denotes better binding affinity of the ligands towards the receptor. The standard EGFR inhibitors **PQ-1** [30,48], Erlotinib, and Gefitinib docked in the receptor with high consensus score (0, 8, 13 respectively). The docking results showed that compounds **7e** and **7f** have high consensus score (50 and 49 respectively) in comparison to other synthesized derivatives. This evidence emphasizes our design strategy about incorporating the pyrazole ring together with the quinolin-2-one scaffold.

Erlotinib interacts in the EGFR receptor with formation of a hydrogen bond (HB; 1.71 Å) towards the ATP-binding site of EGFR coming from pyrimidine-N2 with Met:769:A. This docking mode is similar to the cocrystallized docking pose with the receptor [50].

The lead compound **PQ-1** [32,50] showed good interaction with the EGFR receptor through formation of two HBs with Met:769:A coming from its lactam group (donor and acceptor). Moreover, it participates in HB with Lys:721:A through its phenolic OH group (Fig. 8 A). The most potent derivative (compound **7f)** interacts with the EGFR receptor by formation of HB with Met:769:A through the carbonyl of its quinolinone ring. Moreover, it formed HB with Lys:721:A through the nitrile group (adjacent to the amino functionality) of pyrazole ring (Fig. 8 B). This docking mode demonstrated that both scaffolds, quinolone and pyrazole, participate in essential HB interactions. Interestingly, compound **7e** showed good overlay with the standard Erlotinib (Fig. 8 C). Compound **7e** forms HB with Asp:831:A through the amino group of the pyrazole moiety. Also, it formed two HBs with Thr:830:A through the nitrile functionality which is adjacent to the amino group (Fig. 8 D). This interaction of the amino and ortho nitrile parts with the peptide Thr:830-Asp:831:A looks like a cyclic system.

Table 4
Results of *in vitro* five dose testing of nine human cancer types and selectivity for compounds **7e** and **7f**.

Panel	Cell line	7e					7f				
		GI_{50}			TGI	LC_{50}	GI_{50}			TGI	LC_{50}
		Conc. per cell line	MID[b]	Selectivity ratio			Conc. per cell line	MID[b]	Selectivity ratio		
Leukemia	CCRF-CEM	> 100	–	–	> 100	> 100	> 100	74.2	0.66	> 100	> 100
	HL-60(TB)	> 100			> 100	> 100	> 100			> 100	> 100
	K-562	> 100			> 100	> 100	> 100			> 100	> 100
	MOLT-4	> 100			> 100	> 100	> 100			> 100	> 100
	RPMI-8226	> 100			> 100	> 100	> 100			> 100	> 100
	SR	> 100			> 100	> 100	74.2			> 100	> 100
Non-small cell lung cancer	A549/ATCC	> 100	11.35	3.79	> 100	> 100	v100	22.27	2.21	> 100	> 100
	EKVX	11.5			> 100	> 100	4.60			> 100	> 100
	HOP-62	> 100			> 100	> 100	> 100			> 100	> 100
	HOP-92	11.2			> 100	> 100	> 100			> 100	> 100
	NCI-H226	> 100			> 100	> 100	> 100			> 100	> 100
	NCI-H23	> 100			> 100	> 100	51.5			> 100	> 100
	NCI-H322M	> 100			> 100	> 100	> 100			> 100	> 100
	NCI-H460	> 100			> 100	> 100	> 100			> 100	> 100
	NCI-H522	> 100			> 100	> 100	22.7			86.4	> 100
Colon Cancer	COLO 205	59.3	59.3	0.73	> 100	> 100	> 100	–	–	> 100	> 100
	HCC-2998	> 100			> 100	> 100	> 100			> 100	> 100
	HCT-116	> 100			> 100	> 100	> 100			> 100	> 100
	HCT-15	> 100			> 100	> 100	> 100			> 100	> 100
	HT29	> 100			> 100	> 100	> 100			> 100	> 100
	KM12	> 100			> 100	> 100	> 100			> 100	> 100
	SW-620	> 100			> 100	> 100	> 100			> 100	> 100
CNS Cancer	SF-268	> 100	–	–	> 100	> 100	67.0	65.97	0.74	> 100	> 100
	SF-295	> 100			> 100	> 100	> 100			> 100	> 100
	SF-539	> 100			> 100	> 100	51.7			> 100	> 100
	SNB-19	> 100			> 100	> 100	> 100			> 100	> 100
	SNB-75	> 100			> 100	> 100	57.1			> 100	> 100
	U251	> 100			> 100	> 100	88.1			> 100	> 100
Melanoma	LOX IMVI	> 100	–	–	> 100	> 100	> 100	–	–	> 100	> 100
	MALME-3M	> 100			> 100	> 100	> 100			> 100	> 100
	M14	> 100			> 100	> 100	> 100			> 100	> 100
	MDA-MB-435	> 100			> 100	> 100	> 100			> 100	> 100
	SK-MEL-2	> 100			> 100	> 100	> 100			> 100	> 100
	SK-MEL-28	> 100			> 100	> 100	> 100			> 100	> 100
	SK-MEL-5	> 100			> 100	> 100	> 100			> 100	> 100
	UACC-257	> 100			> 100	> 100	> 100			> 100	> 100
	UACC-62	> 100			> 100	> 100	> 100			> 100	> 100
Ovarian Cancer	IGROV1	> 100	8.63	4.99	> 100	> 100	37.9	37.9	1.29	> 100	> 100
	OVCAR-3	> 100			> 100	> 100	> 100			> 100	> 100
	OVCAR-4	8.63			> 100	> 100	> 100			> 100	> 100
	OVCAR-5	> 100			v100	> 100	> 100			> 100	> 100
	OVCAR-8	> 100			> 100	> 100	> 100			> 100	> 100
	NCI/ADR-RES	> 100			> 100	> 100	> 100			> 100	> 100
	SK-OV-3	> 100			> 100	> 100	> 100			> 100	> 100
Renal Cancer	786-0	> 100	–	–	> 100	> 100	> 100	–	–	> 100	> 100
	ACHN	> 100			> 100	> 100	> 100			> 100	> 100
	CAKI-1	> 100			> 100	> 100	> 100			> 100	> 100
	RXF 393	> 100			> 100	> 100	> 100			> 100	> 100
	SN12C	> 100			> 100	> 100	> 100			> 100	> 100
	UO-31	> 100			> 100	> 100	> 100			> 100	> 100
Prostate Cancer	PC-3	> 100	–	–	> 100	> 100	> 100	–	–	> 100	> 100
	DU-145	> 100			> 100	> 100	> 100			> 100	> 100
Breast Cancer	MCF7	82.3	70.33	0.61	> 100	> 100	64.1	45.15	1.09	> 100	> 100
	MDA-MB-231/ ATCC	89.8			> 100	> 100	> 100			> 100	> 100
	HS 578T	> 100			> 100	> 100	64.9			> 100	> 100
	BT-549	> 100			> 100	> 100	> 100			> 100	> 100
	T-47D	38.9			> 100	> 100	6.46			> 100	> 100
	MDA-MB-468	> 100			> 100	> 100	> 100			> 100	> 100

MID[a] for 7e = 43.09, MID[a] for 7f = 49.19.

2.4. Structure activity relationship

The presence of cyclized pyrazole at position 4 of quinolone gave much better activity than the open scaffold at the same position on the majority of the tested cancer cell lines. This is due to rigidification of pyrazole part to occupy the pocket occupied by the aryl part as shown by the docking pose (Fig. 9). Moreover, it is clear that substitution at quinolone 6-position with electron withdrawing groups like Br or Cl enhances greatly the anticancer activity, while introduction of a 6-methyl group reduces activity greatly. Similarly, shift of the substituent into position 5 of the quinolone moiety abolished activity (cf. **6b** and **6c**) . This is due to increased strength of HB interaction of the amide

Table 5
Antiproliferative activities of compounds **6c-f**, **7b**, **7e** and **7f.**

Compound	Antiproliferative activity IC_{50} ± SEM (μM)	
	MOLT-4	CCRF-CEM
6c	43.19 ± 0.71	12.55 ± 0.06
6d	14.75 ± 0.28	10.32 ± 0.07
6e	11.34 ± 0.22	11.38 ± 0.02
6f	7.57 ± 0.16	16.39 ± 0.32
7b	7.05 ± 0.11	5.42 ± 0.05
7e	4.34 ± 0.14	5.07 ± 0.10
7f	1.35 ± 0.08	2.42 ± 0.04
Erlotinib	7.38 ± 0.56	4.92 ± 0.24

Table 6
Effects of compounds **6e**, **6f**, **7b**, **7e** and **7f** on EGFR TK kinase.

Compound	EGFR IC_{50} (nM)
6e	703.84
6f	472.41
7b	345.19
7e	298.27
7f	247.14
Erlotinib	208.42

Table 7
Effect of compounds **7e**, **7f** and erlotinib on the active caspases-3, 8 and 9 in MOLT-4 cell line.

Compound Number	Caspase-3		Caspase-8		Caspase-9	
	Conc (pg/ml)	Fold change	Conc (ng/ml)	Fold change	Conc (ng/ml)	Fold change
7e	319	5.14	0.48	2.82	24.05	10.10
7f	361	5.82	0.60	3.52	22.94	9.63
Erlotinib	405	6.53	1.11	6.52	26.56	11.15
Control	62	1	0.17	1	02.38	1

Table 8
Bax and Bcl-2 levels for compounds **7e, 7f**, and **erlotinib** on MOLT-4 cells.

Compound Number	Bax		Bcl-2	
	Conc (pg/ml)	Fold change	Conc (ng/ml)	Fold change
7e	249.10	04.89	1.36	03.83
7f	221.80	04.35	1.70	03.06
Erlotinib	251.40	04.94	0.99	05.26
Control	50.88	1	5.21	1

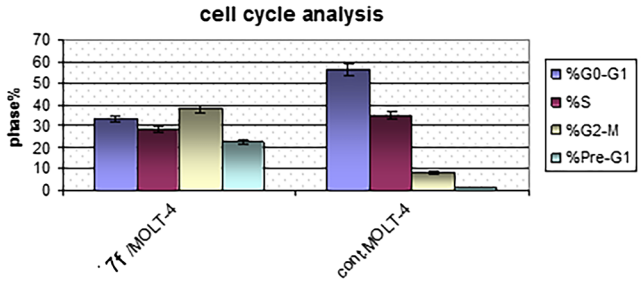

Fig. 5. Cell cycle analysis results for compound **7.**

functionaility in quinolinone ring with the amino acids. Also this separation of the substitutent from exocyclic pyrazole part from the quinolinone ring maintains the same distance as represented in standards (Fig. 9). The most potent compound **7f** interacts with the EGFR receptor

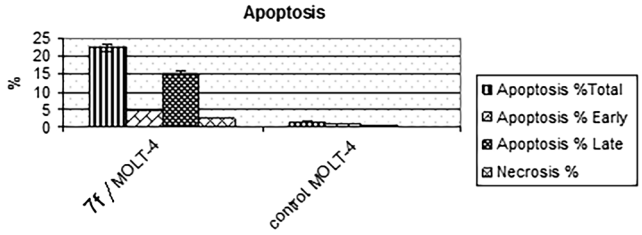

Fig. 6. Apoptosis induction analysis using Annexin V/PI for compound**7f.**

by formation of HB with Met:769:A amino acid through thecarbonyl of its quinolone ring. Moreover, it formed HB with Lys:721:A amino acids through the nitrile group (adjacent to amino functionality) of pyrazole ring.

According to compounds pose and mode shown from docking studies (Figs. 7 and 8), we found that our designed compounds have a resemblance to the reported compounds erlotinib and PQ-1, as illustrated from the graphical representation of the SAR of the most potent series in this work (Fig. 9). The anticancer and activity against EGFR of the target compounds depends on both the two parts constituting the hybrid, the 2-quinolone and pyrazole scaffolds, and also on the nature of the substituent.

3. Conclusion

A new series of 4-pyrazolyl-quinolin-2-ones **7a-f** and the open chain analogues **6a-g** were characterized by different spectroscopic and elemental techniques including IR, ^{1}H NMR, ^{13}C NMR, 2D NMR, MS and elemental microanalyses. *In vitro* one dose anticancer screening results revealed that the cyclized 5-amino-1*H*-pyrazole-3,4-dicarbonitrile derivatives **7a-f** are more potent than the open chain analogues **6a-g**. Compounds **7e** and **7f** were selected for five dose testing against the full panel of 60 human tumor cell lines and compound **7e** showed moderate selectivity against ovarian, small cell lung, leukemia and cancer cell lines. Testing of the most active compounds **7a-f** showed that 6-halogen substituted derivatives **7e** and **7f** are the most active against leukemia MOLT-4 and CCRF-CEM cell lines with IC_{50} = 4.34 ± 0.14 μM and 5.07 ± 0.10 μM (**7e**); 1.35 ± 0.08 μM and 2.42 ± 0.04 μM (**7f**) compared to erlotinib with IC_{50} = 7.38 ± 0.56 μM and 4.92 ± 0.24 μM, respectively.

Compounds **7e** and **7f** experienced an outstanding inhibitory activity comparable to erlotinib on the EGFR TK with IC_{50} = 247.14 nM and 208.42 nM, respectively. Cell cycle analysis indicated cell cycle arrest at G2/M phase (supported by Caspases, BAX and Bcl-2 studies) with a significant pro-apoptotic activity as indicated by annexin V-FITC staining. Moreover, the docking study mode showed that both pyrazole moiety and quinolone ring showed good fitting into EGFR receptor (PDB code: 1 M17). The 2-quinolone-pyrazoles **7e** and **7f** are considered promising lead antiproliferative EGFR TK inhibitors.

4. Experimental

4.1. Chemistry

Melting points were determined using open glass capillaries on a Gallenkamp melting point apparatus (Weiss-Gallenkamp, Loughborough, UK), and are uncorrected. The IR spectra were recorded from potassium bromide disks with a FT device, Minia University. NMR spectra were measured in DMSO-d_6 on a Bruker AV-400 spectrometer (400 MHz for ^{1}H, 100 MHz for ^{13}C, and 40.55 MHz for ^{15}N); chemical shifts are expressed in δ (ppm), versus internal tetramethylsilane (TMS) = 0 for ^{1}H and ^{13}C, and external liquid ammonia = 0 for ^{15}N. Coupling constants are stated in Hz. Correlations were established using ^{1}H–^{1}H COSY, and ^{1}H–^{13}C and ^{1}H-^{15}N HSQC and HMBC experiments. ^{15}N signals were observed indirectly, through the proton channel in

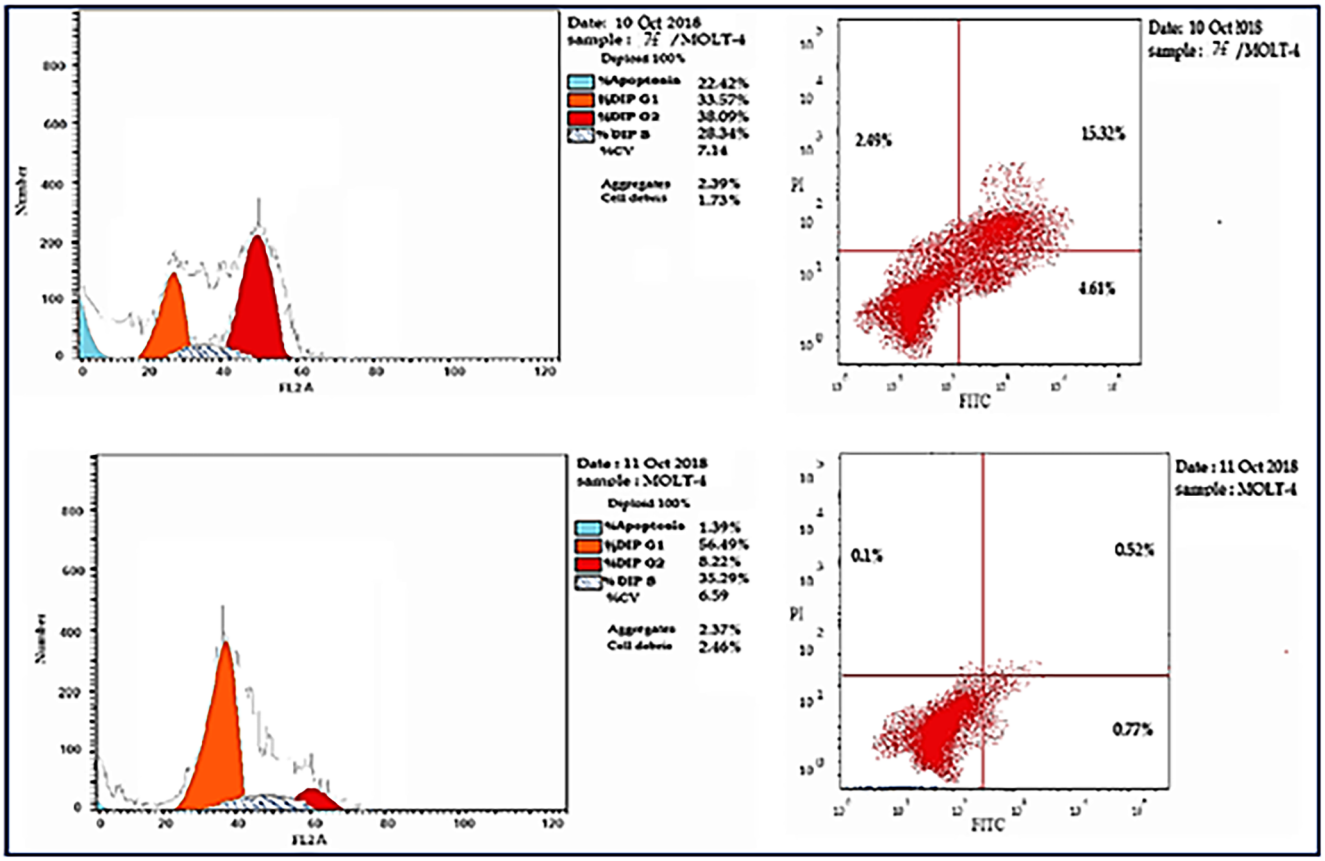

Fig. 7. Apoptosis induction analysis using Annexin V/PI for compound **7f**.

HSQC or HMBC experiments. Mass spectra were recorded on a Finnigan Fab 70 eV, Institute of Organic Chemistry, Karlsruhe University, Karlsruhe, Germany. TLC was performed on analytical Merck 9385 silica aluminum sheets (Kieselgel 60) with Pf_{254} indicator; TLC's were viewed at λ_{max} = 254 nm. Elemental analyses were carried out at the Microanalytical Center, Cairo University, Egypt.

4.2. General details: see Appendix A

4.2.1. General method for the synthesis of compounds 6a-g

To a solution of hydrazino quinolone **5** (1 mmol) in dry DMF (30 mL), diethyl acetylenedicarboxylate (0.17 gm, 1 mmol) was added. The reaction mixture was heated under reflux for 10–16 h (monitored by TLC). After reaction completion, the reaction mixture was poured onto a mixture of crushed ice and water with vigorous stirring. The precipitated solid was filtered, washed with water, dried and crystallized from methanol to afford compounds **6a-g**.

4.2.1.1. Diethyl 2-(2-(2-oxo-1,2-dihydroquinolin-4-yl)hydrazono)succinate (6a). Yield: 0.29 g (84%); mp 190–192 °C, IR (KBr) υ_{max}/cm^{-1} 3291, 2983, 1742, 1655. NMR: Table 1. LCMS: *m/z* calcd: 345.13, found $[M-H]^-$: 344. Anal. Calcd for $C_{17}H_{19}N_3O_5$ (345.13): C, 59.12; H, 5.55 ; N, 12.70. Found: C, 58.89; H, 5.37; N, 12.61.

4.2.1.2. Diethyl 2-(2-(5-methyl-2-oxo-1,2-dihydroquinolin-4-yl)hydrazono) succinate (6b). Yield: 0.28 g (80%); mp 198–200 °C, IR (KBr) υ_{max}/cm^{-1} 3299, 2975, 1743, 1647. ^{1}H NMR δ_H 12.37 (s, 1H: NH-4b), 11.35 (s, 1H; NH-1), 7.37 (t, *J* = 7.6, 1H; H-7), 7.21 (d, *J* = 7.8, 1H; H-8), 6.89 (d, *J* = 7.0 Hz, 1H; H-6), 6.47 (s, 1H; H-3), 4.28 (q, *J* = 6.8 Hz, 2H; H-4j), 4.14 (q, *J* = 6.7 Hz, 2H; H-4 g), 3.63 (s, 2H; H-4e), 2.88 (s, 3H; H-5a), 1.25 (t, *J* = 6.9, 3H; H-4 k), 1.22 (t, *J* = 7.0 Hz, 3H; H-4 h). ^{13}C NMR δ_C 169.85 (C-4f), 161.70, 161.65 (C-2, 4i), 149.36 (C-4), 140.97 (C-8a), 133.30 (C-5), 130.27, 130.10 (C-4d, 7), 125.45 (C-6), 114.73 (C-8), 111.59 (C-4a), 98.73 (C-3), 61.55 (C-4j), 60.55 (C-4 g), 39.16 (C-4e), 23.82 (C-5a), 14.04 (C-4 k), 13.72 (C-4 h). ^{15}N NMR δ_N 343.6 (N-4c), 151.2 (N-4b), 147.0 (N-1). LCMS: *m/z* calcd: 359.15, found $[M+H]^+$: 359.9. Anal. Calcd for $C_{18}H_{21}N_3O_5$ (359.15):C, 60.16; H, 5.89; N, 11.69. Found: C, 60.32; H, 6.08; N, 11.75.

4.2.1.3. Diethyl 2-(2-(6-methyl-2-oxo-1,2-dihydroquinolin-4-yl)hydrazono) succinate (6c). Yield: 0.32 g (90%); mp 221–223 °C, IR (KBr) υ_{max}/cm^{-1} 3307, 2975, 1740, 1647. ^{1}H NMR δ_H 11.31 (s, 1H; NH-1), 10.02 (s, 1H; NH-4b), 7.93 (s, 1H; H-5), 7.37 (d, *J* = 8.3 Hz, 1H; H-7), 7.23 (d, *J* = 8.4 Hz, 1H; H-8), 6.32 (s, 1H; H-3), 4.25 (q, *J* = 7.1 Hz, 2H; H-4j), 4.13 (q, *J* = 7.1 Hz, 2H; H-4 g), 3.97 (s, 2H; H-4e), 2.39 (s, 3H; H-6a), 1.29 (t, *J* = 7.1 Hz, 3H; H-4 k), 1.20 (t, *J* = 7.1 Hz, 3H; H-4 h). ^{13}C NMR δ_C 168.30 (C-4f), 163.95 (C-4i), 162.24 (C-2), 147.91 (C-4), 137.39 (C-8a), 135.11 (C-4d), 131.96 (C-7), 129.80 (C-6), 122.34 (C-5), 115.56 (C-8), 111.84 (C-4a), 99.22 (C-3), 61.02 (C-4j), 60.72 (C-4 g), 32.13 (C-4e), 20.61 (C-6a), 14.09 (C-4 k), 13.98 (C-4 h). ^{15}N NMR δ_N 342.6 (N-4c), 144.3 (N-1), 141.8 (N-4b). LCMS: *m/z* Calcd: 359.15, found $[M+H]^+$: 359.9. Anal. Calcd for $C_{18}H_{21}N_3O_5$ (359.15):C, 60.16; H, 5.89; N, 11.69. Found: C, 60.04; H, 6.13; N, 11.88.

4.2.1.4. Diethyl 2-(2-(6-methoxy-2-oxo-1,2-dihydroquinolin-4-yl)hydrazono) succinate (6d). Obtained as an equally-populated mixture of C=N stereoisomers. Plain numbers denote one isomer, primed numbers the other. Yield 0.28 g (77%), mp 188–189 °C, IR (KBr) υ_{max}/cm^{-1} 3215, 2991, 1738, 1651. ^{1}H NMR δ_H 12.40 (s, 1H; NH-4b′), 11.30 (s, 1H; NH-1, 1′), 10.04 (s, 1H; H-4b), 7.64 (d, *J* = 2.4 Hz, 1H; H-5), 7.32 (d, *J* = 9.0 Hz, 1H; H-8′), 7.29 (d, *J* = 8.9 Hz, 1H; H-8), 7.28 (dd, *J* = 9.0 Hz, 2.4, 1H; H-7′), 7.24 (dd, *J* = 9.0, 2.4 Hz, 1H; H-7), 6.93 (d, *J* = 2.3 Hz, 1H; H-5′), 6.34 (s, 1H; H-3), 6.31 (s, 1H; H-3′), 4.32 (q, *J* = 7.1 Hz, 2H; H-4j′), 4.25 (q, *J* = 7.1 Hz, 2H; H-4j), 4.14 (q, *J* = 7.0 Hz, 2H; H-4 g′), 4.12 (q, *J* = 7.0

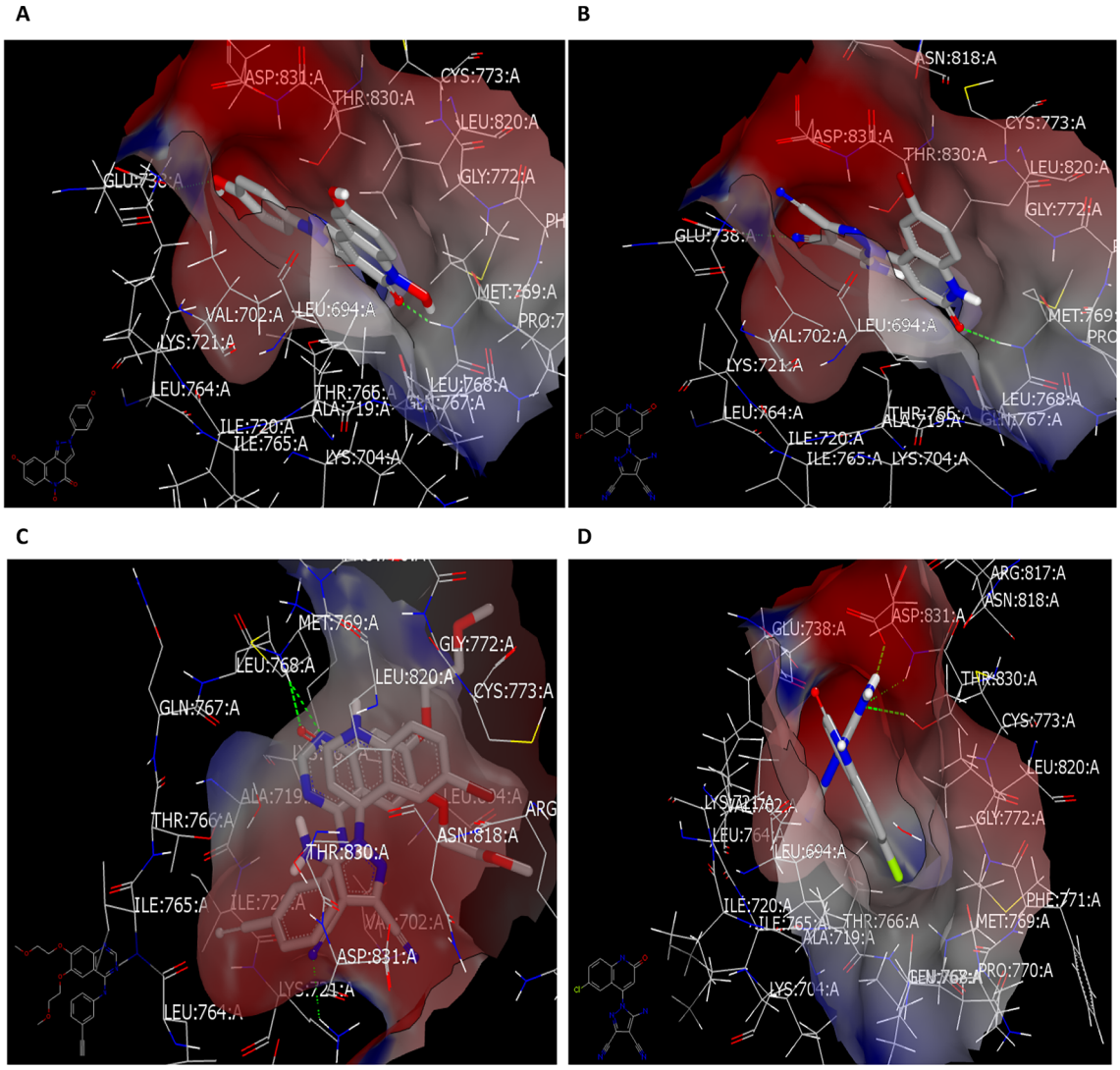

Fig. 8. (A) Visual representation of compound PQ-1 docked with 1M17 (B) Visual representation of **7f** docked with 1M17, showed HB with Met:769:A and Lys:721:A; (C) Visual representation of **7f** overlaid with standard erlotinib, showed HB interactions with the same amino acid Met:769:A; (D) Visual representation of **7e** with formation of HB with Thr:830:A and Asp:831:A.

Hz, 2H; H-4 g), 3.97 (s, 2H; H-4e), 3.83 (s, 3H; H-6a, 6a′), 3.62 (s, 2H; H-4e′), 1.29 (t, J = 7.1 Hz, 3H; H-4 k), 1.28 (t, J = 7.1 Hz, 3H; H-4k′), 1.21 (t, J = 7.0 Hz, 3H), 1.20 (t, J = 7.0 Hz, 3H; H-4 h, 4 h′). ^{13}C NMR δ_C 169.77 (C-4f′), 168.37 (C-4f), 163.94 (C-4i), 162.40, 161.92, 161.87 (C-2, 2′, 4i′), 153.89, 153.56 (C-6, 6′), 147.70 (C-4), 145.75 (C-4′), 135.05 (C-4d), 133.92, 133.89 (C-8a, 8a′), 130.85 (C-4d′), 119.41, 119.13 (C-7, 7′), 117.46, 116.83 (C-8, 8′), 112.46 (C-4a), 111.57 (C-4a′), 106.16 (C-5), 102.75 (C-5′), 99.84 (C-3), 97.34 (C-3′), 61.75 (C-4j′), 61.04 (C-4j), 60.74, 60.59 (C-4g, 4g′), 55.67, 55.44 (C-6a, 6a′), 39.00 (C-4e′), 32.16 (C-4e), 14.09, 14.04 (C-4h, 4h′), 13.98, 13.71 (C-4k, 4k′). ^{15}N NMR δ_N 343.1 (N-4c), 341.6 (N-4c′), 146.1 (N-4b′), 143.1 (N-1, 1′), 142.3 (N-4b). LCMS: *m/z* calcd: 375.14, found [M−H]+: 374.00. Anal. Calcd for $C_{18}H_{21}N_3O_6$ (375.14): C, 57.59; H, 5.64; N, 11.19. Found: C, 57.43; H, 5.80; N, 11.23.

4.2.1.5. Diethyl 2-(2-(6-chloro-2-oxo-1,2-dihydroquinolin-4-yl)hydrazono) succinate (6e). Yield: 0.28 g (74%;), mp 211–213 °C, IR (KBr) υ_{max}/cm^{-1} 3244, 2984, 1741, 1641. ^{1}H NMR δ_H 12.32 (s, 1H; NH-4b), 11.55 (s, 1H; NH-1), 7.64 (dd, J = 8.9, 2.0 Hz, 1H; H-7), 7.49 (d, J = 2.0 Hz, 1H; H-5), 7.37 (d, J = 8.8 Hz, 1H; H-8), 6.34 (s, 1H; H-3), 4.34 (q, J = 7.1 Hz, 2H; H-4j), 4.14 (q, J = 7.1 Hz, 2H; H-4 g), 3.64 (s, 2H; H-4e), 1.29 (t, J = 7.1, 3H Hz; H-4 k), 1.21 (t, J = 7.1 Hz, 3H; H-4 h). ^{13}C NMR δ_C 169.68 (C-4f), 162.19, 162.05 (C-2, 4i), 145.51 (C-4), 138.21 (C-8a), 131.59 (C-4d), 130.94 (C-7), 125.45 (C-6), 119.85 (C-5), 117.8 (C-8), 112.49 (C-4a), 97.75 (C-3), 61.84 (C-4j), 60.61 (C-4g), 39.08 (C-4e), 14.03 (C-4h), 13.71 (C-4k). ^{15}N NMR δ_N 340.3 (N-4c); N-1, 4b not observed. LCMS: *m/z* Calcd: 379.09, found [M−H]+: 378.10. Anal. Calcd for $C_{17}H_{18}ClN_3O_5$ (379.09):C, 53.76; H, 4.78; N, 11.06. Found: C, 53.94; H, 4.91; N, 10.89.

4.2.1.6. Diethyl 2-(2-(6-bromo-2-oxo-1,2-dihydroquinolin-4-yl)hydrazono) succinate (6f). Yield: 0.36 g (86%), mp 215–217 °C, IR (KBr) υ_{max}/cm^{-1} 3328, 2992, 1736, 1675. ^{1}H NMR δ_H 11.52 (s, 1H; NH-1), 10.10 (s, 1H; NH-4b), 8.43 (d, J = 2.0 Hz, 1H; H-5), 7.70 (dd, J = 8.8, 2.1 Hz, 1H; H-7), 7.27 (d, J = 8.8 Hz, 1H; H-8), 6.35 (s, 1H; H-3), 4.25 (q, J = 7.1 Hz, 2H; H-4j), 4.13 (q, J = 7.1 Hz, 2H; H-4g), 3.97 (s, 2H; H-4e), 1.29 (t, J = 7.1 Hz, 3H; H-4k), 1.21 (t, J = 7.1 Hz, 3H; H-4h). ^{13}C NMR δ_C 168.23 (C-4f), 163.90 (C-4i), 162.05 (C-2), 147.35 (C-4), 138.50 (C-8a), 135.62 (C-4d), 133.44 (C-7), 125.43 (C-5), 117.72 (C-8), 113.66 (C-6), 112.91 (C-4a), 100.09 (C-3), 61.08 (C-4j), 60.73 (C-4g), 32.23 (C-4e), 14.10 (C-4k), 14.00 (C-4h). LCMS: *m/z* Calcd: 423.04, found [M−H]+: 422.10. Anal. Calcd for $C_{17}H_{18}BrN_3O_5$ (423.04): C, 48.13; H, 4.28; N, 9.90. Found: C, 48.26; H, 4.47; N, 10.18.

4.2.1.7. Diethyl 2-(2-(1-methyl-2-oxo-1,2-dihydroquinolin-4-yl)hydrazono)

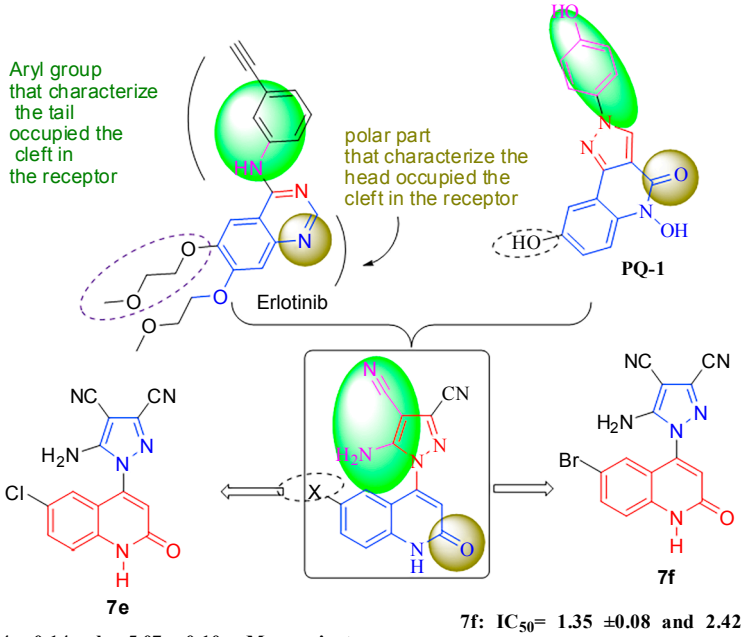

Fig. 9. Graphical representation of the SAR of the most potent of the designed compounds, and standards erlotinib and PQ-1.

succinate (6 g). Yield: 0.26 g (75%); mp: 184–186 °C, IR (KBr) υ_{max}/cm^{-1} 3311, 2984, 1731, 1630. ^{1}H NMR δ_H 10.11 (s, 1H; NH-4b), 8.20 (d, J = 7.8 Hz, 1H; H-5), 7.69 (t, J = 7.3 Hz, 1H; H-7), 7.55 (d, J = 8.5 Hz, 1H; H-8), 7.32 (t, J = 7.5 Hz, 1H; H-6), 6.48 (s, 1H; H-3), 4.26 (q, J = 7.1 Hz, 2H; H-4j), 4.12 (q, J = 7.1 Hz, 2H; H-4 g), 3.98 (s, 2H; H-4e), 3.59 (s, 3H, NCH_3), 1.29 (t, J = 7.1 Hz, 3H; H-4 k), 1.20 (t, J = 7.1 Hz, 3H; H-4 h). ^{13}C NMR δ_C 168.29 (C-4f), 163.93 (C-4i), 161.52 (C-2), 146.98 (C-4), 139.99 (C-8a), 135.53 (C-4d), 131.32 (C-7), 123.32 (C-5), 120.96 (C-6), 115.08 (C-8), 112.99 (C-4a), 98.83 (C-3), 61.06 (C-4j), 60.73 (C-4 g), 32.19 (C-4e), 28.68 (N-CH_3), 14.10 (C-4 k), 13.99 (C-4 h). ^{15}N NMR δ_N 342.3 (N-4c), 140.7 (N-4b), 138.4 (N-1). LCMS: *m/z* calcd: 359.15, found [M−H]+: 358.20. Anal. Calcd for $C_{18}H_{21}N_3O_5$ (359.15): C, 60.16; H, 5.89; N, 11.69. Found: C, 60.33; H, 6.12; N, 11.85.

4.2.2. General method for the synthesis of compounds (7a-f)

A mixture of substituted hydrazino-quinolone compounds **5a-f** (1 mmol) with **TCNE** (0.128 g, 1 mmol) in ethanol (25 mL) was heated under reflux for 20–24 h. After reaction completion (the reaction was followed by TLC analysis), the solvent was removed under vacuum and the residue was washed with diethyl ether and crystallized from ethanol.

4.2.2.1. 5-Amino-1-(2-oxo-1,2-dihydroquinolin-4-yl)-1H-pyrazole-3,4-dicarbonitrile (7a). Yield: 0.18 g (65%), mp 183–185 °C, IR (KBr) υ_{max}/cm^{-1} 3325, 3164, 2222, 1674. ^{1}H NMR δ_H 12.22 (s, 1H; NH-1), 7.61 (t, J = 7.6, 1H; H-7), 7.56 (bs, 2H; NH_2), 7.43 (d, J = 8.2 Hz, 1H; H-8), 7.20 (t, J = 7.6 Hz, 1H; H-6), 7.13 (d, J = 7.9 Hz, 1H; H-3), 6.84 (s, 1H; H-3).^{13}C NMR δ_C 161.26 (C-2), 153.05 (C-5′), 142.71 (C-4), 139.53 (C-8a), 131.67 (C-7), 126.77 (C-3′), 123.59 (C-5), 122.50 (C-3), 122.42 (C-6), 115.82, 115.69 (C-4a, 8), 111.86 (C-3a′, 4a′), 75.69 (C-4′).^{15}N NMR δ_N 188.5 (N-1′), 152.7 (N-1), 62.9 (NH_2); N-2′ and nitrile nitrogens not observed. LCMS: *m/z* calcd: 276.08, found [M−H]+: 275.10. Anal. Calcd for $C_{14}H_8N_6O$ (276.08):C, 60.87; H, 2.92; N, 30.42. Found: C, 60.71; H, 3.17; N, 30.27.

4.2.2.2. 5-Amino-1-(5-methyl-2-oxo-1,2-dihydroquinolin-4-yl)-1H-pyrazole-3,4-dicarbonitrile (7b). Yield: 0.19 g (68%), mp 160–162 °C, IR (KBr) υ_{max}/cm^{-1} 3277, 3168, 2223, 1675. ^{1}H NMR δ_H 12.15 (s, 1H; NH-1), 7.56 (bs, 2H; NH_2), 7.24 (t, J = 7.5 Hz, 1H; H-7), 7.14 (d, J = 7.8 Hz, 1H; H-8), 6.84 (d, J = 7.2 Hz, 1H; H-6), 6.73 (s, 1H; H-3), 2.72 (s, 3H; H-5a).^{13}C NMR δ_C 161.46 (C-2), 152.97 (C-5′), 142.73 (C-4), 139.69 (C-8a), 134.34 (C-5), 126.72 (C-3′), 124.63 (C-7), 123.86, 123.46 (C-3, 6), 115.34, 114.05, 112.07, 111.86 (C-3a′, 4a, 4a′, 8), 75.67 (C-4′), 23.62 (C-5a). LCMS: *m/z* calcd: 290.09, found [M−H]+: 289.10. Anal. Calcd for $C_{15}H_{10}N_6O$ (290.09):C, 62.06; H, 3.47; N, 28.95. Found: C, 62.13; H, 3.66; N, 28.89.

4.2.2.3. 5-Amino-1-(6-methyl-2-oxo-1,2-dihydroquinolin-4-yl)-1H-pyrazole-3,4-dicarbonitrile (7c). Yield: 0.21 g (75%), mp 210–212 °C, IR (KBr) υ_{max}/cm^{-1} 3349, 3166, 2223, 1647. ^{1}H NMR δ_H 12.16 (s, 1H; NH-1), 7.53 (bs, 2H; NH_2), 7.44 (d, J = 8.9 Hz, 1H; H-7), 7.34 (d, J = 7.6 Hz, 1H; H-8), 6.92 (s, 1H; H-5), 6.78 (s, 1H; H-3), 2.30 (s, 3H; H-6a).^{13}C NMR δ_C 161.12 (C-2), 152.98 (C-5′), 142.56 (C-4), 137.63 (C-8a), 132.97 (C-7), 131.69 (C-6), 126.75 (C-3′), 122.74 (C-5), 122.47 (C-3), 115.80, 115.68 (C-4a, 8), 111.94 (C-3a′, 4a′), 75.72 (C-4′), 20.39 (C-6a). ^{15}N NMR δ_N 189.0 (N-1′), 152.1 (N-1), 62.7 (NH_2); N-2′ and nitrile nitrogens not observed. LCMS: *m/z* calcd: 290.09, found [M−H]+: 289.10. Anal. Calcd for $C_{15}H_{10}N_6O$ (290.09): C, 62.06; H, 3.47; N, 28.95. Found: C, 61.87; H, 3.61; N, 28.82.

4.2.2.4. 5-Amino-1-(6-methoxy-2-oxo-1,2-dihydroquinolin-4-yl)-1H-pyrazole-3,4-dicarbonitrile (7d). Yield: 0.15 g (50%); mp: 183–185 °C, IR (KBr) υ_{max}/cm^{-1} 3347, 3196, 2227, 1674. NMR: Table 2. LCMS: *m/z* calcd: 306.09, found [M−H]+: 305.10. Anal. Calcd for $C_{15}H_{10}N_6O_2$ (306.09): C, 58.82; H, 3.29; N, 27.44. Found: C, 59.14; H, 3.40; N, 27.69.

4.2.2.5. 5-Amino-1-(6-chloro-2-oxo-1,2-dihydroquinolin-4-yl)-1H-pyrazole-3,4-dicarbonitrile (7e). Yield: 0.24 g (78%), mp 196–198 °C, IR (KBr) υ_{max}/cm^{-1} 3359, 3180, 2221, 1648. ^{1}H NMR δ_H 12.34 (s, 1H; NH-1), 7.67 (dd, J = 9.4 Hz, 1.8, 1H; H-7), 7.56 (bs, 2H; NH_2), 7.44 (d, J = 6.4 Hz, 1H; H-8), 7.25 (d, J = 2.4 Hz, 1H; H-5), 6.91 (s, 1H; H-3). ^{13}C NMR δ_C 161.03 (C-2), 153.09 (C-5′), 141.74 (C-4), 138.38 (C-8a), 131.70 (C-7), 127.19, 126.52 (C-3′, 6), 123.77 (C-3), 122.72 (C-5),

117.68 (C-4a), 116.99 (C-8), 111.93, 111.90 (C-3a′, 4a′), 76.05 (C-4′).^{15}N NMR δ_N 187.6 (N-1′), 152.6 (N-1), 63.2 (NH_2); N-2′ and nitrile nitrogens not observed. LCMS: *m/z* Calcd: 310.04, found [M − H] +: 309.00. Anal. Calcd for $C_{14}H_7ClN_6O$ (310.04): C, 54.12; H, 2.27; N, 27.05. Found: C, 54.26; H, 2.40; N, 26.87.

4.2.2.6. 5-Amino-1-(6-bromo-2-oxo-1,2-dihydroquinolin-4-yl)-1H-pyrazole-3,4-dicarbonitrile (7f). Yield: 0.24 g (70%); mp: 217–219 °C, IR (KBr) υ_{max}/cm^{-1} 3361, 3179, 2221, 1648. ^{1}H NMR δ_H 12.34 (s, 1H; NH-1), 7.78 (d, J = 9.4 Hz, 1H; H-7), 7.57 (bs, 2H; NH_2), 7.37 (m, 2H; H-5, 8), 6.89 (s, 1H; H-3).^{13}C NMR δ_C 161.01 (C-2), 153.09 (C-5′), 141.66 (C-4), 138.65 (C-8a), 134.39 (C-7), 127.19 (C-3′), 125.59 (C-5), 123.72 (C-3), 117.90 (C-8), 117.43 (C-4a), 114.24 (C-6), 111.93, 111.90 (C-3a′, 4a′), 76.06 (C-4′). ^{15}N NMR δ_N 187.6 (N-1′), 153.0 (N-1), 62.7 (NH_2); N-2′ and nitrile nitrogens not observed. LCMS: *m/z* Calcd: 353.99, found $[M-H]^{-+}$: 353.00. Anal. Calcd for $C_{14}H_7BrN_6O$ (353.99): C, 47.35; H, 1.99; N, 23.66. Found: C, 47.61; H, 2.17; N, 23.84.

4.3. Biological evaluation

4.3.1. NCI screening assay

As mentioned, the methodology of the NCI procedure for primary anticancer assay was detailed on their site (http://www.dtp.nci.nih.gov). But briefly, the protocol performed at sixty human tumor cell lines panel derived from nine different neoplastic diseases. NCI-60 testing is performed in two parts: first, a single concentration is tested in all 60 cell lines at a single dose of 10^{-5} M or 15 μg/ml in accordance with the protocol of the Drug Evaluation Branch, National Cancer Institute, Bethesda, USA. If the results obtained meet selection criteria, then the compound is tested again in all 60 cell lines in 5 × 10 folds of dilution with the top dose being 10^{-4} M or 150 μg/ml. Detailed methods are described in supplementary material related to this article.

4.3.2. MTT assay for cell viability

To investigate the effect of the newly synthesized compounds on leukemia cancer cells; MTT assay was performed against MOLT-4 and CCRF-CEM cell lines [40] (See Appendix A).

4.3.3. EGFR inhibitory assay

EGFR assay was performed by established reported method using (BPS EGFR Kinase Assay Kit Catalog # 40321 bps bioscience U.S) [41] for selected synthetic compounds **6d, 6f, 7b, 7e** and **7f**. Details are summarized in Appendix A.

4.3.4. Cell cycle analysis and apoptotic assay

4.3.4.1. Cell apoptosis and apoptotic detection. Studies on the effect of compound **7f** on cell cycle development and induction of apoptosis in the MOLT-4 was done using the Annexin V-FITC Apoptosis Detection Kit (BioVision Research Products, USA) [46]. For more details see Appendix A.

4.3.4.2. Activation of caspases. For deeper and more systematic investigation on cell apoptosis, the effect of compounds **7e** and **7f** on caspases-3, 8 and 9 was evaluated and compared to erlotinib as a reference drug; details are summarized in Appendix A.

4.3.4.3. Effects on BAX and Bcl-2 proteins. The activities of compounds **7e** and **7f** against Bcl2 and BAX using MOLT-4 cell line and erlotinib as a reference were investigated according to literature. See Appendix A.

4.3.5. Docking studies

This was done using Open Eye molecular Modeling software [50,51]. Complete details were put in the supplementary information. Appendix A.

Acknowledgement

Purchase of the NMR spectrometer at Florida Institute of Technology was assisted by the National Science Foundation (CHE 03 42251).

Appendix A. Supplementary material

Supplementary data to this article can be found online at https://doi.org/10.1016/j.bioorg.2019.103045.

References

[1] S.M. Prajapati, K.D. Patel, R.H. Vekariya, S.N. Panchal, H.D. Patel, Recent advances in the synthesis of quinolines: a review, RSC Adv. 4 (2014) 24463–24476.
[2] O. Navneetha, K. Deepthi, A.M. Rao, T.S. Jyostna, A review on chemotherapeutic activities of quinoline, Int. J. Pharm. Chem. Biol. Sci. 7 (2017) 364–372.
[3] F. Barlési, C. Tchouhadjian, C. Doddoli, P. Villani, L. Greillier, J.P. Kleisbauer, P. Thomas, P. Astoul, Gefitinib (ZD1839, Iressa®) in non-small-cell lung cancer: a review of clinical trials from a daily practice perspective, Fund. Clin. Pharmacol. 19 (2005) 385–393.
[4] R. Iyer, A. Bharthuar, A review of erlotinib–an oral, selective epidermal growth factor receptor tyrosine kinase inhibitor, Exp. Opin. Pharmacother. 11 (2010) 311–320.
[5] B. Bao, C. Mitrea, P. Wijesinghe, L. Marchetti, E. Girsch, R.L. Farr, J.L. Boerner, R. Mohammad, G. Dyson, S.R. Terlecky, A. Bollig-Fischer, Treating triple negative breast cancer cells with erlotinib plus a select antioxidant overcomes drug resistance by targeting cancer cell heterogeneity, Sci. Rep. 7 (2017) 44125.
[6] J. Stamos, M.X. Sliwkowski, C. Eigenbrot, Structure of the epidermal growth factor receptor kinase domain alone and in complex with a 4-anilinoquinazoline inhibitor, J. Biol. Chem. 277 (2002) 46265–46272.
[7] A. Wissner, D.M. Berger, D.H. Boschelli, M.B. Floyd, L.M. Greenberger, B.C. Gruber, B.D. Johnson, N. Mamuya, R. Nilakantan, M.F. Reich, R. Shen, H.-R. Tsou, E. Upeslacis, Y.F. Wang, B. Wu, F. Ye, N. Zhang, 4-Anilino-6,7-dialkoxyquinoline-3-carbonitrile inhibitors of epidermal growth factor receptor kinase and their bioisosteric relationship to the 4-anilino-6,7-dialkoxyquinazoline inhibitors, J. Med. Chem. 43 (2000) 3244–3256.
[8] A. Wissner, T.S. Mansour, The development of HKI-272 and related compounds for the treatment of cancer, Arch. Pharm. (Weinheim) 341 (2008) 465–477.
[9] B.F. Kiesel, R.A. Parise, A. Wong, K. Keyvanjah, S. Jacobs, J.H. Beumer, LC–MS/MS assay for the quantitation of the tyrosine kinase inhibitor neratinib in human plasma, J. Pharm. Biomed. Anal. 134 (2017) 130–136.
[10] F. Pisaneschi, Q.-D. Nguyen, E. Shamsaei, M. Glaser, E. Robins, M. Kaliszczak, G. Smith, A.C. Spivey, E.O. Aboagye, Development of a new epidermal growth factor receptor positron emission tomography imaging agent based on the 3-cyanoquinoline core: synthesis and biological evaluation, Bioorg. Med. Chem. 18 (2010) 6634–6645.
[11] S. Lü, W. Zheng, L. Ji, Q. Luo, X. Hao, X. Li, F. Wang, Synthesis, characterization, screening and docking analysis of 4-anilinoquinazoline derivatives as tyrosine kinase inhibitors, Eur. J. Med. Chem. 61 (2013) 84–94.
[12] D. Luethi, S. Durmus, A.H. Schinkel, J.H.M. Schellens, J.H. Beijnen, R.W. Sparidans, Liquid chromatography–tandem mass spectrometry assay for the EGFR inhibitor pelitinib in plasma, J. Chromatogr. B 934 (2013) 22–25.
[13] V.G. Pawar, M.L. Sos, H.B. Rode, M. Rabiller, S. Heynck, W.A.L. van Otterlo, R.K. Thomas, D. Rauh, Synthesis and biological evaluation of 4-anilinoquinolines as potent inhibitors of epidermal growth factor receptor, J. Med. Chem. 53 (2010) 2892–2901.
[14] A. Mrozek-Wilczkiewicz, E. Spaczynska, K. Malarz, W. Cieslik, M. Rams-Baron, V. Kryštof, R. Musiol, Design, synthesis and in vitro activity of anticancer styrylquinolines. The p53 independent mechanism of action, PloS One 10 (2015) e0142678.
[15] F.-S. Chang, W. Chen, C. Wang, C.-C. Tzeng, Y.-L. Chen, Synthesis and antiproliferative evaluations of certain 2-phenylvinylquinoline (2-styrylquinoline) and 2-furanylvinylquinoline derivatives, Bioorg. Med. Chem. 18 (2010) 124–133.
[16] N. Jiang, X. Zhai, T. Li, D. Liu, T. Zhang, B. Wang, P. Gong, Design, synthesis and antiproliferative activity of novel 2-substituted-4-amino-6-halogenquinolines, Molecules 17 (2012) 5870–5881.
[17] G.M. Nitulescu, C. Draghici, O.T. Olaru, L. Matei, A. Ioana, L.D. Dragu, C. Bleotu, Synthesis and apoptotic activity of new pyrazole derivatives in cancer cell lines, Bioorg. Med. Chem. 23 (2015) 5799–5808.
[18] J.B. Shi, W.J. Tang, X.B. Qi, R. Li, X.H. Liu, Novel pyrazole-5-carboxamide and pyrazole–pyrimidine derivatives: synthesis and anticancer activity, Eur. J. Med. Chem. 90 (2015) 889–896.
[19] T.S. Reddy, H. Kulhari, V.G. Reddy, V. Bansal, A. Kamal, R. Shukla, Design, synthesis and biological evaluation of 1,3-diphenyl-1*H*-pyrazole derivatives containing benzimidazole skeleton as potential anticancer and apoptosis inducing agents, Eur. J. Med. Chem. 101 (2015) 790–805.
[20] S.S. Abd El-Karim, M.M. Anwar, N.A. Mohamed, T. Nasr, S.A. Elseginy, Design, synthesis, biological evaluation and molecular docking studies of novel benzofuran–pyrazole derivatives as anticancer agents, Bioorg. Chem. 63 (2015) 1–12.
[21] J.D. Bhatt, C.J. Chudasama, K.D. Patel, Pyrazole clubbed triazolo[1,5-*a*]pyrimidine hybrids as an anti-tubercular agents: synthesis, in vitro screening and molecular

docking study, Bioorg. Med. Chem. 23 (2015) 7711–7716.
[22] X.J. Song, Y. Shao, X.G. Dong, Microwave-assisted synthesis of some novel fluorinated pyrazolo[3,4-*d*]pyrimidine derivatives containing 1,3,4-thiadiazole as potential antitumor agents, Chin. Chem. Lett. 22 (2011) 1036–1038.
[23] M.C. Bagley, M. Baashen, V.L. Paddock, D. Kipling, T. Davis, Regiocontrolled synthesis of 3- and 5-aminopyrazoles, pyrazolo[3,4-*d*]pyrimidines, pyrazolo[3,4-*b*]pyridines and pyrazolo[3,4-*b*]quinolinones as MAPK inhibitors, Tetrahedron 69 (2013) 8429–8438.
[24] M.M. El-Enany, M.M. Kamel, O.M. Khalil, H.B. El-Nassan, Synthesis and antitumor activity of novel 6-aryl and 6-alkylpyrazolo[3,4-*d*]pyrimidin-4-one derivatives, Eur. J. Med. Chem. 45 (2010) 5286–5291.
[25] I. Koca, A. Özgür, K.A. Coşkun, Y. Tutar, Synthesis and anticancer activity of acyl thioureas bearing pyrazole moiety, Bioorg. Med. Chem. 21 (2013) 3859–3865.
[26] C.B. Nanthakumar, R.J.D. Hatley, S. Lemma, J. Gauldie, R.P. Marshall, S.J.F. MacDonald, Dissecting fibrosis: therapeutic insights from the small-molecule toolbox, Nat. Rev. Drug Disc. 14 (2015) 693–720.
[27] S. Verstovsek, R.A. Mesa, J. Gotlib, R.S. Levy, V. Gupta, J.F. DiPersio, J.V. Catalano, M.W. Deininger, C.B. Miller, R.T. Silver, M. Talpaz, E.F. Winton, J.H. Harvey, M.O. Arcasoy, E.O. Hexner, R.M. Lyons, A. Raza, K. Vaddi, W. Sun, W. Peng, V. Sandor, H. Kantarjian, Efficacy, safety, and survival with ruxolitinib in patients with myelofibrosis: results of a median 3-year follow-up of COMFORT-I, Haematologica 100 (2015) 479–488.
[28] P.M. Forde, C.M. Rudin, Crizotinib in the treatment of non-small-cell lung cancer, Exp. Opin. Pharmacother. 13 (2012) 1195–1201.
[29] P.J. Roberts, Clinical use of crizotinib for the treatment of non-small cell lung cancer, Biol.: Targets Ther. 7 (2013) 91–101.
[30] M.S. Christodoulou, S. Liekens, K.M. Kasiotis, S.A. Haroutounian, Novel pyrazole derivatives: synthesis and evaluation of anti-angiogenic activity, Bioorg. Med. Chem. 18 (2010) 4338–4350.
[31] C.H. Jin, M. Krishnaiah, D. Sreenu, K.S. Rao, V.B. Subrahmanyam, C.-Y. Park, J.-Y. Son, Y.Y. Sheen, D.-K. Kim, Synthesis and biological evaluation of 1-substituted-3(5)-(6-methylpyridin-2-yl)-4-(quinolin-6-yl)pyrazoles as transforming growth factor-β type 1 receptor kinase inhibitors, Bioorg. Med. Chem. 19 (2011) 2633–2640.
[32] E.M. El-Sheref, A.A. Aly, A.-F.E. Mourad, A.B. Brown, S. Bräse, M.E.M. Bakheet, Synthesis of pyrano[3,2-*c*]quinoline-4-carboxylates and 2-(4-oxo-1,4-dihydro-quinolin-3-yl)fumarates, Chem. Pap. 72 (2018) 181–190, https://doi.org/10.1007/s11696-017-0269-6.
[33] A.A. Aly, E.M. El-Sheref, A.-F.E. Mourad, A.B. Brown, S. Bräse, M.E.M. Bakheet, M. Nieger, Synthesis of spiro[indoline-3,4'-pyrano[3,2-c]quinolone]-3'-carbonitriles, Monatsh. Chem. 149 (2018) 635–644, https://doi.org/10.1007/s00706-017-2078-6.
[34] A.A. Aly, E.M. El-Sheref, A.-F.E. Mourad, S. Bräse, M.E.M. Bakheet, M. Nieger, One-pot synthesis of 2,3-bis(4-hydroxy-2-oxo-1,2-dihydroquinolin-3-yl)succinates and aryl methylene-bis-3,3'-quinoline-2-ones, Chem. Pap. 73 (2019) 27–37, https://doi.org/10.1007/s11696-018-0561-0.
[35] A.A. Aly, E.M. El-Sheref, M.E.M. Bakheet, M.A.E. Mourad, A.B. Brown, S. Bräse, M. Nieger, M.A.A. Ibrahim, Synthesis of novel 1,2-bis-quinolinyl-1,4-naphthoquinones: ERK2 inhibition, cytotoxicity and molecular docking studies, Bioorg. Chem. 81 (2018) 700–712, https://doi.org/10.1016/j.bioorg.2018.09.017.
[36] A.A. Aly, E.M. El-Sheref, M.E.M. Bakheet, M.A.E. Mourad, S. Bräse, M.A.A. Ibrahim, M. Nieger, B.K. Garvalov, K.N. Dalby, T.S. Kaoud, Design, synthesis and biological evaluation of fused naphthofuro[3,2-c]quinoline-6,7,12-triones and pyrano[3,2-c]quinoline-6,7,8,13-tetraones derivatives as ERK inhibitors with efficacy in BRAF-mutant melanoma, Bioorg. Chem. 82 (2019) 290–305, https://doi.org/10.1016/j.bioorg.2018.10.044.
[37] M. Abass, Chemistry of substituted quinolinones. Part II. Synthesis of novel 4-pyrazolylquinolinone derivatives, Synth. Commun. 30 (2000) 2735–2757.
[38] M.M. Ismail, M. Abass, M.M. Hassan, Chemistry of substituted quinolinones. Part VI. Synthesis and nucleophilic reactions of 4-chloro-8-methylquinolin-2(1*H*)-one and its thione analogue, Molecules 5 (2000) 1224–1239.
[39] M. Ismail, M. Abdel-Megid, M.M. Hassan, Some reactions of 2-and 4-substituted 8-methylquinolin-2(1*H*)-ones and their thio analogues, Chem. Pap. 58 (2004) 117–125.
[40] A.A. Aly, M.A.A. Ibrahim, E.M. El-Sheref, A.M.A. Hassan, A.B. Brown, Prospective new amidinothiazoles as leukotriene B4 inhibitors, J. Mol. Struct. 1175 (2019) 414–427, https://doi.org/10.1016/j.molstruc.2018.07.085.
[41] W. Sucrow, Reactions of acetylenes with hydrazines, Org. Prep. Proc. Int. 14 (1982) 91–155, https://doi.org/10.1080/00304948209354896.
[42] H.-L. Qin, J. Leng, B.G.M. Youssif, M.W. Amjad, M.A.G. Raja, M.A. Hussain, Z. Hussain, S.N. Kazmi, S.N.A. Bukhari, Synthesis and mechanistic studies of curcumin analog-based oximes as potential anticancer agents, Chem. Biol. Drug Des. 90 (2017) 443–449.
[43] F. Manetti, G.A. Locatelli, G. Maga, S. Schenone, M. Modugno, S. Forli, F. Corelli, M. Botta, A combination of docking/dynamics simulations and pharmacophoric modeling to discover new dual c-Src/Abl kinase inhibitors, J. Med. Chem. 49 (2006) 3278–3286.
[44] D.R. McIlwain, T. Berger, T.W. Mak, Caspase functions in cell death and disease, Cold Spring Harbor Perspect. Biol. 5 (2013) a008656.
[45] E.A. Prokhorova, G.S. Kopeina, I.N. Lavrik, B. Zhivotovsky, Apoptosis regulation by subcellular relocation of caspases, Sci. Rep. 8 (2018) 12199.
[46] A. Shamas-Din, J. Kale, B. Leber, D.W. Andrews, Mechanisms of action of Bcl-2 family proteins, Cold Spring Harbor Perspect. Biol. 5 (2013) a008714.
[47] K.J. Campbell, S.W.G. Tait, Targeting BCL-2 regulated apoptosis in cancer, Open Biol. 8 (2018) 180002.
[48] M.H. Abdelrahman, A.S. Aboraia, B.G.M. Youssif, B.E.M. Elsadek, Design, synthesis and pharmacophoric model building of new 3-alkoxymethyl/3-phenyl indole-2-carboxamides with potential antiproliferative activity, Chem. Biol. Drug Des. 90 (2017) 64–82.
[49] J.H. Park, Y. Liu, M.A. Lemmon, R. Radhakrishnan, Erlotinib binds both inactive and active conformations of the EGFR tyrosine kinase domain, Biochem. J. 448 (2012) 417–423.
[50] OpenEye Scientific Software Fast Rigid Exhaustive Docking (FRED) Receptor, version 2.2.5 < http://www.eyesopen.com > .
[51] Y.A.M.M. Elshaier, M.A. Shaaban, M.K. Abd El Hamid, M.H. Abdelrahman, M.A. Abou-Salim, S.M. Elgazwi, F. Halaweish, Design and synthesis of pyrazolo[3,4-*d*]pyrimidines: nitric oxide releasing compounds targeting hepatocellular carcinoma, Bioorg. Med. Chem. 25 (2017) 2956–2970.